Author(s)	Hilder, Leonard O.; Geer, Richard G.
Title	Extension of the root-locus technique into three dimensions
Publisher	Monterey, California: U.S. Naval Postgraduate School
Issue Date	1964
URL	http://hdl.handle.net/10945/12191

EXTENSION OF THE ROOT LOCUS
TECHNIQUE INTO THREE DIMENSIONS

LEONARD O. HILDER, JR.
AND
RICHARD G. GEER

EXTENSION OF THE ROOT-LOCUS

TECHNIQUE INTO THREE DIMENSIONS

by

Leonard O. Hilder, Jr.

Lieutenant Commander, United States Navy

and

Richard G. Geer

Lieutenant, United States Navy

EXTENSION OF THE ROOT-LOCUS

TECHNIQUE INTO THREE DIMENSIONS

by

Leonard O. Hilder, Jr.

and

Richard G. Geer

This work is accepted as fulfilling

the thesis requirements for the degree of

MASTER OF SCIENCE

IN

ELECTRICAL ENGINEERING

from the

United States Naval Postgraduate School

ABSTRACT

The root-locus technique used in the determination of system response has been a powerful tool for the engineer. Shortcomings of the technique, however, particularly in regard to the locations of imaginary roots and the frequency stability of the system for changes in the system gain, have made a supplementary technique desirable. Such a technique utilizing the projection onto the K- $j\omega$ plane of the three-dimensional root-locus has been developed. The use of the root-locus plot in conjunction with the K- $j\omega$ trace eliminates these shortcomings and provides the engineer with still another tool in his quest for a more complete method of systems analysis.

TABLE OF CONTENTS

LIST OF TABLES

LIST OF ILLUSTRATIONS

TABLE OF SYMBOLS AND ABBREVIATIONS

G — the forward transfer function

H — the feedback transfer function

GH — the open-loop transfer function

s — the complex Laplacian variable

σ — the real part of s

j — $\sqrt{-1}$

ω — the imaginary part of s

K — the system root-locus gain

K_{EMERG} — the value of K at a point on the s-plane where the root-locus departs the σ-axis

K_{ENT} — the value of K at a point on the s-plane where the root-locus enters the σ-axis

$\sum$ — summation symbol

n — the number of excess poles of a given transfer function

P — pole

Z — zero

$\triangleq$ — definition symbol

$\equiv$ — "identically equal to" symbol

X(s) — Laplace Transform of input function

Y(s) — Laplace Transform of output function

x — general variable

INTRODUCTION

For many years engineers have been using root-locus methods of solving high-order polynominal characteristic equations of control systems. As an example, consider the simple servo system shown in Fig. 1.1.
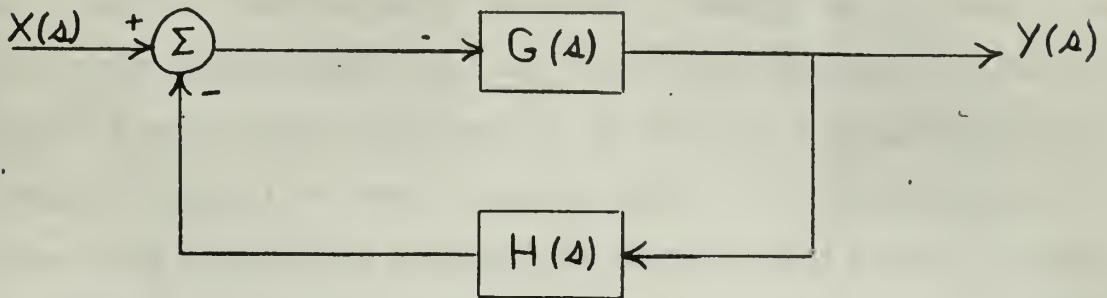
SIMPLE FEEDBACK CONTROL SYSTEM
Fig. 1.1

In general, the blocks G and H represent any pole-zero combinations which might describe the system. The characteristic equation of the system is

$$1 + GH = 0 \; ,$$

which can be written in general terms as

$$s^m (s + P_{G1})(s + P_{G2}) \cdots (s + P_{H1})(s + P_{H2}) \cdots +$$
$$K(s + Z_{G1})(s + Z_{G2}) \cdots (s + Z_{H1})(s + Z_{H2}) \cdots = 0,$$

1.1

where   n = 1, 2, 3, - - -

K = root-locus gain

P_G = pole of G

P_H = pole of H

Z_G = zero of G

Z_H = zero of H

s = Laplacian variable $\triangleq \sigma + j\omega$

Obviously, equation 1.1 could be a polynominal of any order, and the
analytic solution of this equation becomes tedious and impractical as
n increases. Consequently, the root-locus method of solution based upon
the pole-zero configuration of the open-loop transfer function GH, which
is both simple and straightforward, has been widely used in engineering
practice. Such a plot provides a wealth of information about the system
in question and is relatively easy and quick to obtain. There are, how-
ever, certain shortcomings to the method. Notably, the root-locus plot
of a given system response does not permit ready evaluation of the loca-
tions of roots of the characteristic equation for a given value of the
root-locus gain, K, or over a specific range of K. A trial and error
measurement procedure is required, and for very small K where the roots
lie close to the poles, this graphical method usually fails completely.
In addition, there is no information concerning sensitivity of the system
to changes in gain.

The first of these shortcomings has been partially resolved by Dr.
R. C. H. Wheeler, of the U. S. Naval Postgraduate School. Substituting
$\Delta = \sigma + j\omega$ into equation 1.1 and letting $j\omega = 0$, Dr. Wheeler was able to
obtain a plot of K vs. σ (called the "Wheeler plot"). With the Wheeler
plot, the _real_ roots of the characteristic equation can be determined,
if they exist, for any value of the root-locus gain. The most valuable
contribution of the Wheeler plot was the prediction of a maximum or a
minimum value of K for those σ at which the root-locus emerges from or
enters the σ-axis. Thus, the value of K at these points, called K_{EMERG}
and K_{ENT}, respectively, may be quickly determined from the root-locus
plot without the necessity for plotting the Wheeler plot. An example
of the Wheeler plot is shown in Fig. 1.2 for the open-loop transfer
function, GH $= \dfrac{K(\Delta+2)}{\Delta(\Delta+1)}$.

2
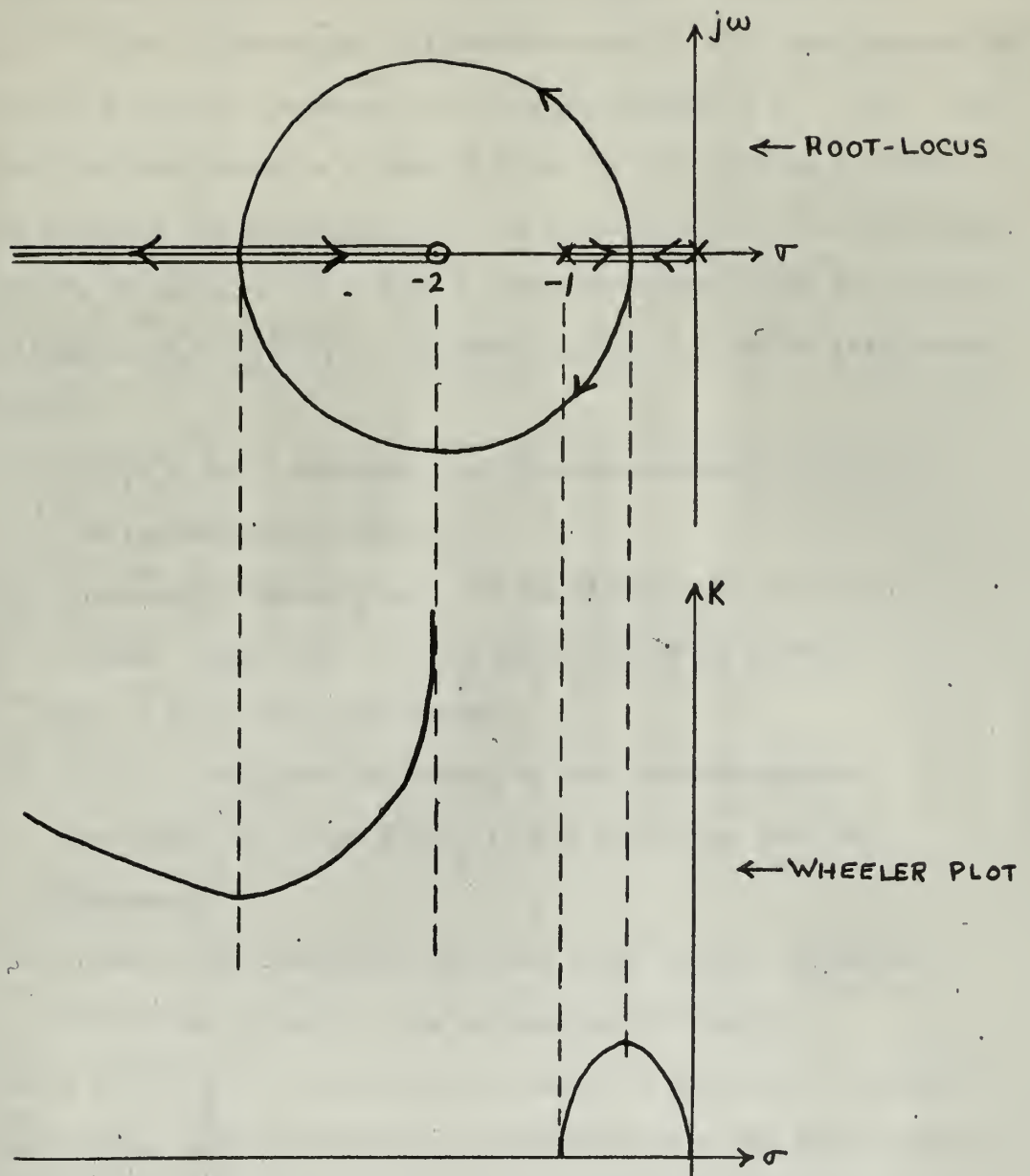
ROOT-LOCUS AND WHEELER PLOTS FOR GH = $\frac{K(s+2)}{s(s+1)}$ FOR $K \geq 0$.

ARROWS DENOTE INCREASING K.

Fig. 1.2

3

However, no information is available from the Wheeler plot concerning complex roots, nor even about the real parts of such complex roots.

Returning to equation 1.1 as the first step in searching for answers to these shortcomings, the substitution of $\Delta = \sigma + j\omega$ immediately revealed this to be an equation in the three variables, σ, $j\omega$, and K. Since the root-locus is a plot of σ vs. $j\omega$ for varying K, such a plot is actually the projection upon the $\sigma - j\omega$ plane of the three-dimensional plot of equation 1.1.. Such a three-dimensional plot for the previous example, $GH = \dfrac{K(\Delta+2)}{\Delta(\Delta+1)}$, is shown in Fig. 1.3 and is interpreted as follows:

1) Curves B and C represent the three-dimensional plot of the characteristic equation.

2) Curve B, for which $j\omega = 0$, is the Wheeler plot for the system. This curve is identical to the plot shown in Fig. 1.2 for this same system.

3) Curve A, being the projection of the three-dimensional curve upon the $\sigma - j\omega$ plane, is the root-locus plot for the system.

4) Curve D, the projection upon the $K - j\omega$ plane, is called the "$K - j\omega$ trace" in the succeeding development.

Curve D of Fig. 1.3 showed great promise of providing a solution to the shortcomings mentioned previously connected with the root-locus plot: the imaginary part of any complex root is immediately available for any value of K, and the frequency stability for varying K is obvious by inspection over any given range of K. The problem, then, became that of determining whether the $K - j\omega$ trace for any given system could be

4
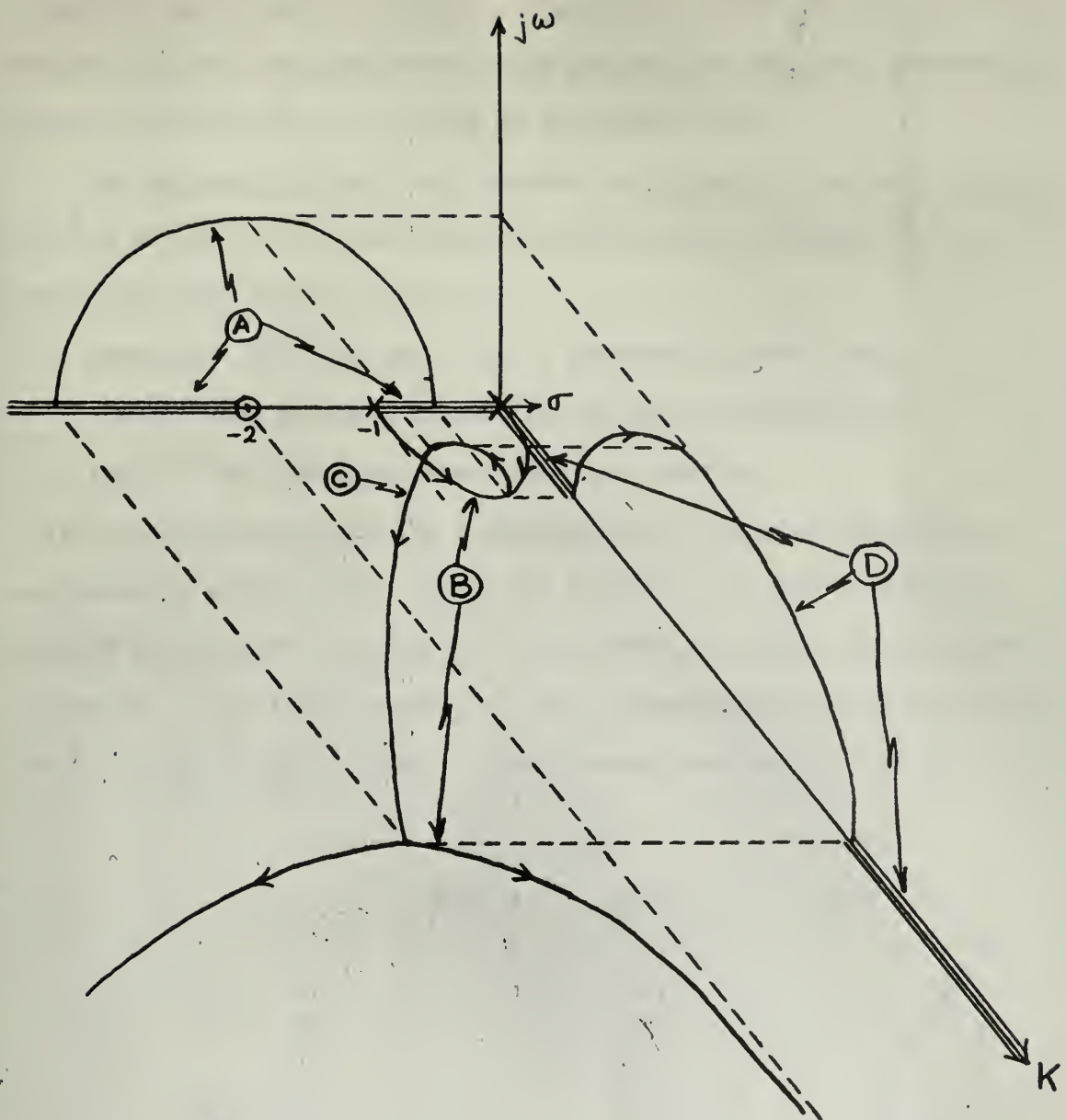
THREE-DIMENSIONAL PLOT OF $1 + GH = 0$ FOR $GH = \dfrac{K(\Delta+2)}{\Delta(\Delta+1)}$

FOR $K \geq 0$ AND FOR $j\omega \geq 0$. ARROWS DENOTE

INCREASING K.

Fig. 1.3

5

sketched quickly and accurately. Speed and ease of sketching were

paramount requirements; otherwise, a graphical trial and error pro-

cedure utilizing the root-locus would provide the required information

without the necessity for making an additional plot.

Two methods of attack were pursued in seeking a solution to the

problem of rapidly and accurately sketching the $K - j\omega$ trace for any

given open-loop transfer function:

METHOD I: The location of poles and zeros on the K-axis

through some suitable transformation upon the poles and

zeros of the given open-loop transfer function.

In searching for a suitable transformation to use, an independent

variable, M, in the $K - j\omega$ plane was defined as follows: $M \triangleq K + j\omega$

where M was a vector in the $K - j\omega$ plane from the origin to any point

$(K, j\omega)$ on the $K - j\omega$ trace. M, then, corresponded to the Laplacian

vector, s, in the $\sigma - j\omega$ plane. These vectors are depicted in Fig. 1.4.
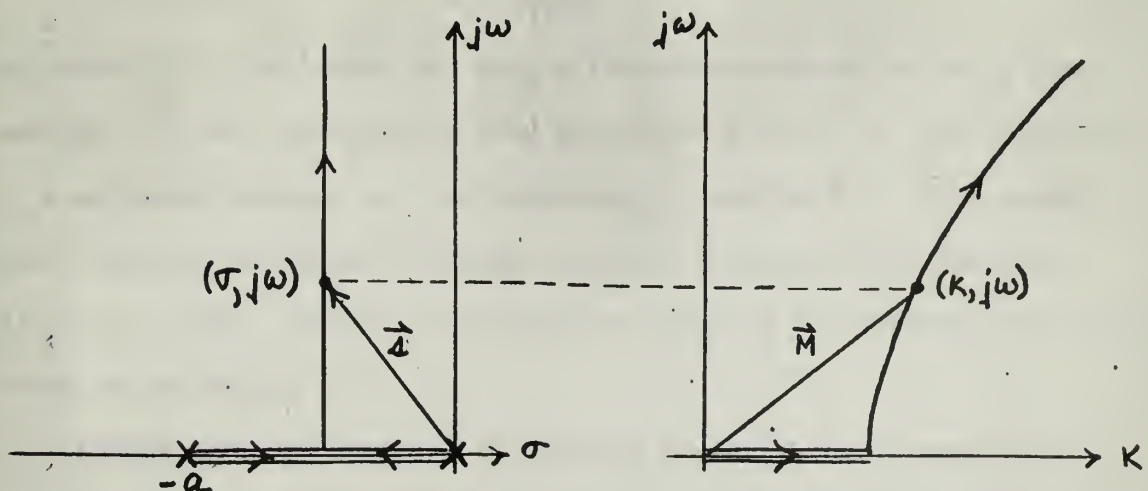
ROOT-LOCUS PLOT AND $K - j\omega$ TRACE FOR GH $= \dfrac{K}{s(s+a)}$ FOR $K \geq 0$ AND

$j\omega \geq 0$ SHOWING THE RELATIONSHIP BETWEEN THE VECTORS $\vec{s}$ AND $\vec{M}$.

Fig. 1.4

The attempt was then made to express the open-loop transfer function in the form

$$GH = \frac{\sigma(M+a)(M+b)\dots}{M^n(M+A)(M+B)\dots}$$

1.2

where small letters denote zeros on the K-axis, capital letters (except M) denote poles on the K-axis, and n represents the system "type" when the transformation has been completed. This method broke down immediately, however, as soon as it was attempted with the simplest second-order system, $GH = \frac{k}{\Delta^2}$. Substituting $\Delta = \sigma + j\omega$ into the equation $1 + GH = 0$ resulted in

$$\sigma^2 + (j\omega)^2 + K + j\,2\sigma\omega = 0$$

1.3

Inspection of equation 1.3 revealed the impracticability of separating M and obtaining the desired form of GH. This can be seen more clearly by dividing equation 1.3 by $K + (j\omega)^2$, resulting in

$$GH = \frac{\sigma(\sigma + j2\omega)}{k + (j\omega)^2} = -1$$

1.4

Equation 1.4, then, shows the two difficulties encountered using this method: 1) the inability to form the vector M, and 2) the inability to completely separate out the independent variable σ . This method was attempted on several different transfer functions with the same (and often worse) result. Consequently, method I for obtaining the $K-j\omega$ trace was abandoned.

METHOD II: The location of critical points on the K-axis such that a set of rules similar to those used for making a root-locus plot might be established for sketching the $K - j\omega$ trace.

7

Basically, this method involved looking at the projection of the three-dimensional curve of the characteristic equation upon the $K - j\omega$ plane. From this projection, then, critical points were established as appeared most promising for the system under consideration. Although the results in some cases were slightly different than anticipated, the use of this method provided a successful solution to the problem of obtaining the $K - j\omega$ trace quickly and accurately. For the case of characteristic equations in the form of second-order polynomials, the $K - j\omega$ trace was determined analytically - the development for this case is traced through in chapter II. For characteristic equations in the form of third or higher order polynomials, an approximate graphical method of obtaining the $K - j\omega$ trace was developed as shown in chapter III.

Utilizing method II, therefore, it was shown that the $K - j\omega$ trace for _any_ given open-loop transfer function can be sketched quickly and accurately using the concepts developed in the succeeding two chapters.

8

SECOND-ORDER SYSTEMS

2.1 <u>DISCUSSION</u>. For the purpose of this development, a second-order system is defined as a system having a characteristic equation in the form of a polynomial of degree less than or equal to two. For such a system, a relatively easy <u>analytic</u> solution to both the root-locus plot and the $K - j\omega$ trace was obtained.

The Laplacian variable,- $s = \sigma + j\omega$, is a vector whose variable components (in the mathematical sense) are σ and ω , with $j = \sqrt{-1}$ being a 90° rotation of the ω -axis from the σ -axis. In engineering practice, however, the variables are usually taken to be σ and $j\omega$ --- hence, the term "K- $j\omega$ trace". Although this term is used throughout this paper, the second variable will be ω rather than $j\omega$ for purposes of the mathematical development in this chapter, although the variable <u>plotted</u> will be $j\omega$. Elsewhere in this paper, $j\omega$ will be used as the variable in accordance with accepted engineering practice. The illustrations shown in this chapter will be plotted only for positive values of K, since negative values of K result in a 0° root-locus. The K-$j\omega$ trace for negative values of K is discussed in chapter III.

As a general second-order system, the open-loop transfer function, $GH = \dfrac{k(A\Delta^2 + B\Delta + C)}{D\Delta^2 + E\Delta + F}$, was used for this development.

2.2 <u>ROOT-LOCUS PLOT</u>.[1] The characteristic equation, 1 + GH = 0, of the general second-order system became:

$$(D + AK)\Delta^2 + (E + BK)\Delta + F + CK = 0.$$

---

[1] Although this is not a new concept, the work was original and necessary for the development of the K- $j\omega$ trace following in section 2.3.

Substituting $s = \sigma + j\omega$ resulted in the equation,

$$\left[(D+AK)\sigma^2 - (D+AK)\omega^2 + (E+BK)\sigma + F+CK\right] + j\omega\left[2(D+AK)\sigma + E+BK\right] = 0.$$

Noting that this equation was in the vector form, $\alpha + j\beta = 0$, it followed that $\alpha = 0$ and $\beta = 0$. Writing these expressions explicitly yielded the pair of equations,

$$(D+AK)\sigma^2 - (D+AK)\omega^2 + (E+BK)\sigma + F+CK = 0 \qquad 2.1$$

and

$$\omega\left[2(D+AK)\sigma + E+BK\right] = 0. \qquad 2.2$$

The reason for using ω as the third variable now becomes evident: equations 2.1 and 2.2 are the parametric form of the characteristic equation and therefore are the parametric form of the <u>curve</u> of the characteristic equation. These equations, of course, were obtained only under the assumption that the characteristic equation could be written in <u>vector</u> form, which necessitated using ω as the variable. Equation 2.1, with $\omega = 0$, is the equation of the Wheeler plot. For this condition (i.e., $\omega = 0$) the root-locus is easily determined as well as the Wheeler plot, and no further investigation of this condition was deemed necessary.

For the condition $\omega \neq 0$, however, the root-locus is not so easily determined, and the Wheeler plot is not defined. Now, the root-locus plot becomes a <u>projection</u> of the three-dimensional curve of the characteristic equation upon the $\sigma - j\omega$ plane. From equation 2.2 it was evident that $\omega \neq 0$ implied the variables σ and K could be determined in terms of each other, yielding:

10

$$K = -\frac{2D\tau + E}{2A\tau + B} \qquad\qquad 2.3$$

and

$$\tau = -\frac{E + BK}{2(D + AK)} \qquad\qquad 2.4$$

The projection of the three-dimensional curve upon the $\tau - j\omega$ plane, then, was obtained by substituting equation 2.3 into equation 2.1. Performing this substitution, collecting terms and completing the square in τ resulted in the equation,

$$\left[\tau + \frac{AF - CD}{AE - BD}\right]^2 + \omega^2 = \frac{CE - BF}{AE - BD} + \left[\frac{AF - CD}{AE - BD}\right]^2. \qquad 2.5$$

Clearly, equation 2.5 is the equation of a <u>circle</u> centered at

$$\tau = -\frac{AF - CD}{AE - BD}, \qquad \omega = 0$$

with radius

$$R = \sqrt{\frac{CE - BF}{AE - BD} + \left[\frac{AF - CD}{AE - BD}\right]^2}.$$

It was concluded that the portion of the root-locus plot for which $\omega \neq 0$ for all second-order systems is a circle. This circle can be determined exactly by using equation 2.5 in conjunction with the coefficients of the open-loop transfer function with two exceptions:

1) For an open-loop transfer function containing no zeros, $A = B = 0$, and equation 2.5 no longer applies. Returning to equations 2.1 and 2.2 in this case, the circle is degenerate into a straight line given by

$$\tau = -\frac{E}{2D}.$$

2) For an open-loop transfer function having a pole-zero configuration resulting in poles separated by zero (s), or vice-versa, there is no root-locus for $\omega \neq 0$.

11

Open-loop transfer functions with pole-zero configurations resulting in the applicability of the foregoing two exceptions present no difficulty in quickly sketching an accurate root-locus plot. The root-locus plot for all other second-order systems may also be quickly and accurately sketched by substituting the coefficients of the numerator and denominator polynomials of the open-loop transfer function into equation 2.3 to determine the center and radius of the required circle.
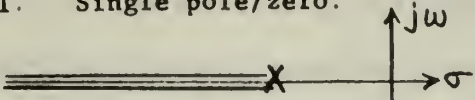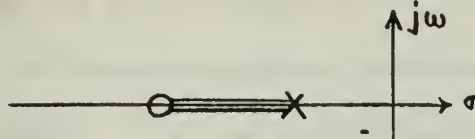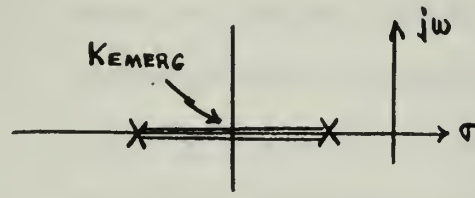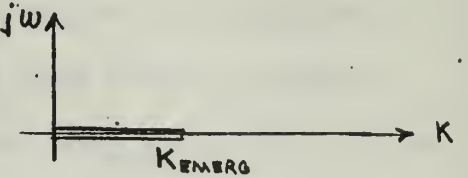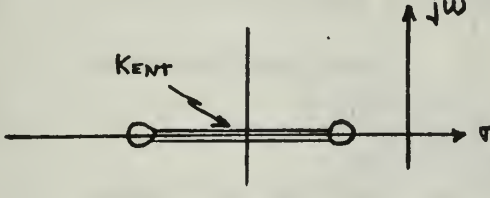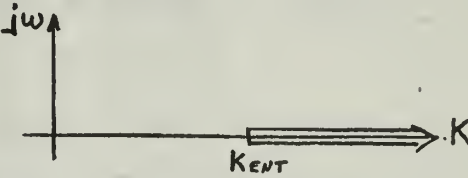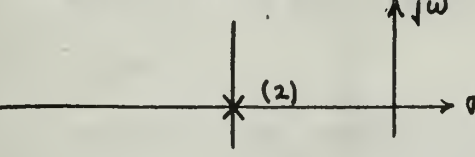
2.3 <u>K-$j\omega$ TRACE.</u>[1] The K-$j\omega$ trace was developed in two parts: the portion for which $\omega = 0$, and the remainder for which $\omega \neq 0$.

For $\omega = 0$, the K-$j\omega$ trace must lie entirely on the K-axis. Since the Wheeler plot is the K-σ plot for $\omega = 0$, the K-$j\omega$ trace for $\omega = 0$ must be simply the projection of the Wheeler plot into the K-axis. From a knowledge of the Wheeler plot, then, the K-$j\omega$ trace for $\omega = 0$ can be determined from the real pole-zero configuration of the open-loop transfer function as shown in Table 2.1.

Following the same procedure for $\omega \neq 0$ which was used for the root-locus development in section 2.2, equation 2.4 was substituted into the equation $\alpha = 0$, resulting in:

$$(B^2 - 4AC)K^2 + 2(BE - 2AF - 2CD)K + 4D^2\omega^2 + 8ADK\omega^2 + 4A^2K^2\omega^2 = 4DF - E^2 \qquad 2.6$$

[1] When the term "K" is used in conjunction with the "K-$j\omega$ trace", it is inferred to be the <u>root-locus gain</u> of the open-loop transfer function. In general, this will also be the gain of $GH = \frac{K(As^2 + Bs + C)}{Ds^2 + Es + F}$ because $A = D = 1$,
if both coefficients are present in any given open-loop transfer function. These coefficients are utilized in this development solely to allow the second-order terms in the open-loop transfer function to go to zero in special cases.

12

REAL POLE-ZERO CONFIGURATION	$K-j\omega$ TRACE ON K-AXIS
I. Single pole/zero.	Entire K-axis.
II Pole-zero combination (with root-locus on the σ-axis between the pole and the zero).	
III. Pole-Pole combination (with root locus on the σ-axis between the poles).	K-axis from the origin to K_{EMERG}
IV. Zero-Zero combination (with root-locus on the σ-axis between the zeros).	K-axis from K_{ENT} to infinity.
V Double pole/zero.	None.

REAL PART OF $K-j\omega$ TRACE FOR CERTAIN OPEN-LOOP POLE-ZERO CONFIGURATIONS

Table 2.1

Immediately, difficulty in obtaining a simple, analytic solution was
encountered, because equation 2.6 is <u>NOT</u> the equation of a simple conic
section. The term $8ADK\omega^2$ suggests a cubic, and the term $4A^2K^2\omega^2$
suggests a quartic equation. An analytic solution of the quartic equa-
tion 2.6, although possible, would not yeild an "easy" method of deter-
mining the K-$j\omega$ trace.

Two possible graphical methods of solution of equation 2.6 were
considered: (1) the "partitioning" method, and (2) an "approximation"
method.

(1) "<u>Partitioning</u>" method. The method has been generally
described elsewhere as follows: any polynomial (up to
about fifth degree) can be "partitioned" by dividing the
entire polynomial by one or more terms of the polynomial,
yielding an equation in root-locus form, i.e., GH =-1, where
GH is some combination of poles and zeros multiplied by some
variable. For example, the polynomial

$$x^4 + bx^3 + cx^2 + dx + e = 0$$

can be partitioned by dividing by ($x^4 + bx^3$), yielding
the root-locus form,

$$\frac{c\left(x^2 + \frac{d}{c}x + \frac{e}{c}\right)}{x^3(x^4 + b)} = -1,$$

where c is the "root-locus" variable. In order to use
this method, the original characteristic equation was
utilized, and ($j\omega$) was considered as the third variable,
yielding

$$D\sigma^2 + AK\sigma^2 + D(j\omega)^2 + E\sigma + BK\sigma + F + CK + 2D\sigma(j\omega) + 2AK\sigma(j\omega) + E(j\omega)$$
$$+ BK(j\omega) = 0 \qquad\qquad 2.7$$

14

Difficulty was immediately encountered due to the presence of the cross-variable terms, and no amount of juggling would enable the "root-locus" variable, σ, to be separated in such a manner that the "root-locus form" of equation 2.7 could be written. Basically, this method required the defining of a new vector $M \triangleq K + j\omega$, to provide a correspondence to the Laplacian variable in the root-locus plot, as was shown in chapter I. Inspection of equation 2.7 shows why this method could not be adopted - the required separation of variables could not be achieved.

(2) "Approximation" method. Returning to the general second-order open-loop transfer function,

$$GH = \frac{K(A\sigma^2 + B\sigma + C)}{D\sigma^2 + E\sigma + F}$$

the denominator was divided into the numerator, resulting in

$$GH = \frac{KA}{D} + \frac{K(B'\sigma + C')}{D\sigma^2 + E\sigma + F} \qquad 2.8$$

where $B' = B - \frac{AE}{D}$ and $C' = C - \frac{AF}{D}$. Defining $(GH)' \triangleq \frac{K(B'\sigma + C')}{D\sigma^2 + E\sigma + F}$, it was noted that $(GH)'$ had the appearance of an open-loop transfer function similar to GH, the only difference being the number and positions of the zeros. Furthermore, $1 + (GH)' = 0$ was known to yield the equation of an ellipse in the $K\text{-}j\omega$ plane! This was proved by returning to equation 2.6:

The two cross-variable terms both involved the coefficient A. Since the presence of

15

these terms precluded equation 2.6 from repre-
senting a conic section, their elimination (by
setting A = 0) would result in the desired conic
section. Performing this operation, collecting
terms and completing the square in K resulted in
the equation

$$\frac{\left[K - \frac{2CD - BE}{B^2}\right]^2}{\frac{4D}{B^4}(B^2F - BCE + C^2D)} + \frac{\omega^2}{\frac{1}{D}(B^2F - BCE + C^2D)} = 1.$$

2.9

By inspection, equation 2.9 is the equation of
an <u>ellipse</u> centered at $\left[K = \frac{2CD - BE}{B^2}, \quad \omega = 0\right]$
with semi-axes given by $\sqrt{\frac{B^2F - BCE + C^2D}{D}}$ and
$\frac{2}{B^2}\sqrt{D(B^2F - BCE + C^2D)}$.

Since (GH)$'$ yielded an ellipse in the K-$j\omega$ plane, the
relationship between GH and (GH)$'$ was determined in an
effort to obtain information about the K-$j\omega$ trace result-
ing from GH. This was accomplished by returning to the
root-locus plots for the two transfer functions, since
both plots must yield circles:

The root-locus plot of GH was a circle having a
center and radius as defined in equation 2.5. Plugging
these formulae with A = 0, B = B$'$ and C = C$'$ resulted
in the center and radius of the circle for (GH)$'$ as
$\left[\nabla a - \frac{C'}{B'}, \quad \omega = 0\right]$ and $R' = \sqrt{\frac{C'E - B'F}{B'D} + \left[\frac{C'}{B'}\right]^2}$.
Substituting $B' = B - \frac{AE}{D}$ and $C' = C - \frac{AF}{D}$, it was
found that the center and radius of the circle for
(GH)$'$ <u>expressed in terms of the variables of GH</u> were

16

identical to the center and radius of the circle for
GH! This is shown graphically in Fig. 2.1. The basic
relationship between GH and (GH)$'$ can be seen by in-
spection of Fig. 2.1. The effect of the division per-
formed to obtain (GH)$'$ was to move the zero at $\bar{z}_1$ to
the center of the circle and the zero at $\bar{z}_2$ to in-
finity. The root-loci of the two functions for $\omega \neq 0$
are identical in shape and position, the only difference
being the values of the root-locus gains at correspond-
ing points on the circles.

With this correspondence established, it was inferred
that the K-$j\omega$ trace for GH must be in the shape of some
sort of "stretched" ellipse with the same maximum ω as
that for the true ellipse of (GH)$'$. To quickly sketch
the K-$j\omega$ trace for GH, then, it would be sufficient to
determine the key points given by $K_{EMERG} \triangleq$ the value of
the root-locus gain for which the root-locus departs the
σ-axis, $K_{ENT} \triangleq$ the value of the root-locus gain for
which the root-locus enters the σ-axis, and $K_{MAX} \triangleq$ the
value of the root-locus gain at the peak (maximum ω) of
the root-locus circle. Since K_{EMERG} and K_{ENT} must both
lie on the K-axis, and since the value of ω corresponding
to K_{MAX} is known from the radius of the root-locus circle,
the key points of the K-$j\omega$ trace are determined. K_{EMERG}
and K_{ENT} are quickly available from the Wheeler plot, and
K_{MAX} is equally quickly available by a simple measurement
on the root-locus plot. With these key points, then, and

17
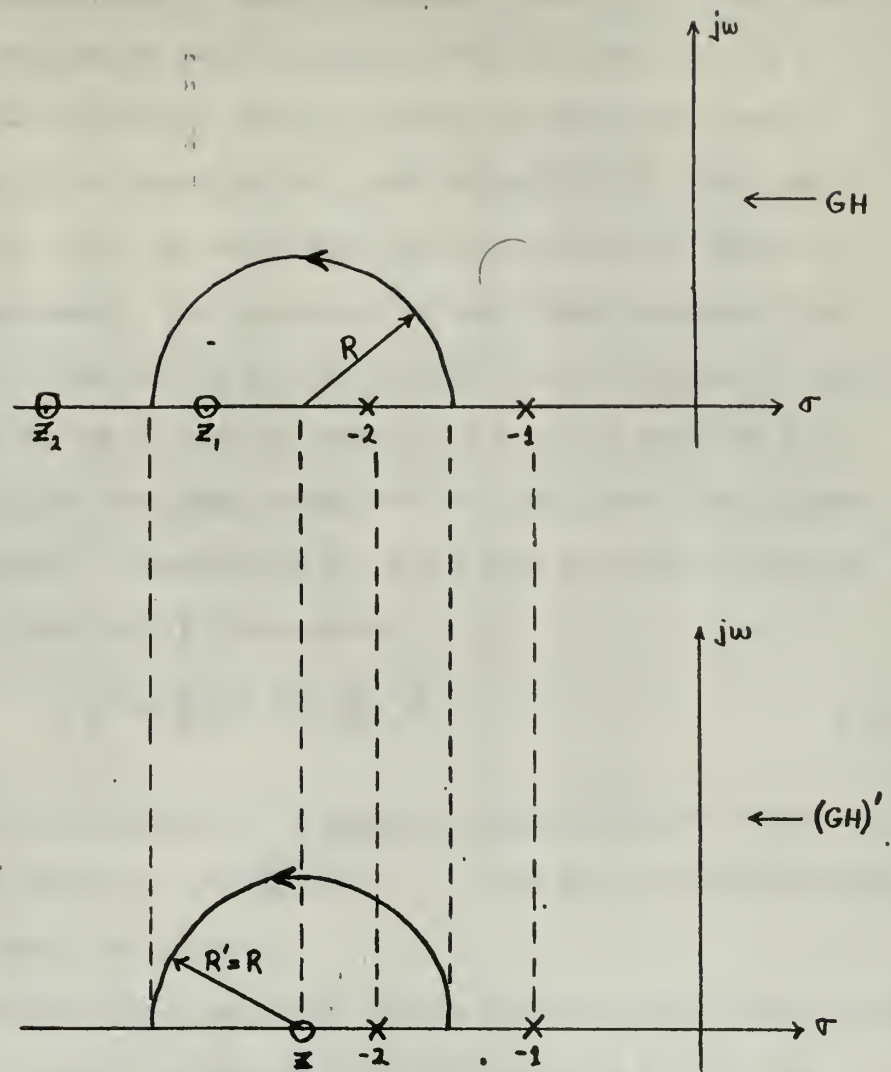
ROOT-LOCUS PLOTS FOR GH AND (GH)′ FOR GH = $\dfrac{K(s+\bar{z}_1)(s+\bar{z}_2)}{(s+1)(s+2)}$, $K \geqslant 0$

AND $j\omega > 0$.

Fig. 2.1

18

knowing the general shape of the curve, the K-$j\omega$ trace
can be quickly sketched.

For the special case in which GH contains no zeros, neither equation
2.9 nor the approximation method provide a valid solution to the K-$j\omega$
trace. This was intuitively obvious, because an open-loop transfer
function containing no zeros yields a root-locus plot for $\omega \neq 0$ which
is an OPEN curve, i.e., the curve does not close on itself except at
infinity. Consequently, the projection of the three-dimensional curve
onto the K-$j\omega$ plane should also be an open curve. Further, it must be
a conic section as may be seen by setting A = B = 0 in equation 2.6.
The K-$j\omega$ trace for this case, then, must be a straight line, a para-
bola or a hyperbola. Substituting A = B = 0 into equation 2.6 and re-
arranging terms resulted in the equation

$$\omega^2 = \frac{C}{D}\left[K + \left(\frac{E}{C} - \frac{E^2}{4CD}\right)\right].$$ 2.10

Equation 2.10 is the equation of a parabola symmetrical with respect to
the K-axis with vertex at [K = $\frac{E^2}{4CD}$ $-\frac{F}{C}$, $\omega = 0$], thus substantiating
the intuitive result anticipated.

It was concluded that the K-$j\omega$ traces for all second-order systems
may be obtained quickly and accurately utilizing Table 2.1 for the
portions for which $\omega = 0$ and Table 2.2 for the portions for which $\omega \neq 0$.

19

OPEN-LOOP TRANSFER FUNCTION	SHAPE OF K-$j\omega$ TRACE	METHOD OF OBTAINING
ALTERNATING POLES AND ZEROS	STRAIGHT LINE (K-AXIS)	PROJECTION OF WHEELER PLOT
NO ZEROS	PARABOLA	EQUATION 2.10
1 ZERO	ELLIPSE	EQUATION 2.9
2 ZEROS	"STRETCHED" ELLIPSE	APPROXIMATION METHOD

SHAPE OF K-$j\omega$ TRACE FOR VARIOUS OPEN-LOOP POLE-ZERO
CONFIGURATIONS, $\omega \neq 0$.

Table 2.2

2.4 **EXAMPLES.** Four examples were selected to illustrate the various

solutions for the root-locus plot and the K-$j\omega$ trace for second-order

systems.

1. $GH = \dfrac{K(s+1)(s+3)}{s(s+2)}$

This is the case of alternating poles and zeros, and the plots are

shown in Fig. 2.2.

2. $GH = \dfrac{K}{(s+1)(s+2)} = \dfrac{K}{s^2+3s+2} \Rightarrow A=B=0, C=D=1, E=3, F=2.$

The root-locus plot for $\omega \neq 0$ is a straight line parallel to the

$j\omega$ -axis and passing through the point $\sigma = -\frac{3}{2}$. The K-$j\omega$ trace

is a parabola symmetrical with respect to the K-axis with vertex

at [K $=\frac{9}{4}-2 = \frac{1}{4}$, $\omega = 0$]. These curves are shown in Fig. 2.3.

3. $GH = \dfrac{K(s+5)}{(s+1)(s+2)} = \dfrac{K(s+5)}{s^2+3s+2} \Rightarrow A=0, B=D=1, C=5, E=3, F=2.$

The root-locus plot is a circle centered at ($\sigma = -5$, $\omega = 0$)

with radius $R = \sqrt{\dfrac{15-2}{-1} + (5)^2} = 2\sqrt{3} = 3.464.$

20

The K-$j\omega$ trace is an ellipse centered at (K = $\frac{10-3}{1}$ = 7,

ω = 0) with (semi-axis)$_K$ = $2\sqrt{2-15+25}$ = $4\sqrt{3}$ = 6.928 and

(semi-axis)$_{j\omega}$ = $\sqrt{12}$ = 3.464. These are plotted in Fig. 2.4.

4. $GH = \frac{K(s+3)(s+4)}{(s+1)(s+2)} = \frac{K(s^2+7s+12)}{s^2+3s+2} \Rightarrow A=D=1, B=7, C=12, E=3, F=2.$

The root-locus plot is a circle centered at ($\sigma = -\frac{2-12}{3-7}$ = -2.5,

ω = 0) with radius R = $\sqrt{\frac{36-14}{3-7} + (2.5)^2}$ = $\sqrt{0.75}$ = 0.867.

The K-$j\omega$ trace is a "stretched" ellipse with key points K_{EMERG} =

0.0718, K_{ENT} = 13.92, K_{MAX} = 1.0. These curves are plotted in

Fig. 2.5.

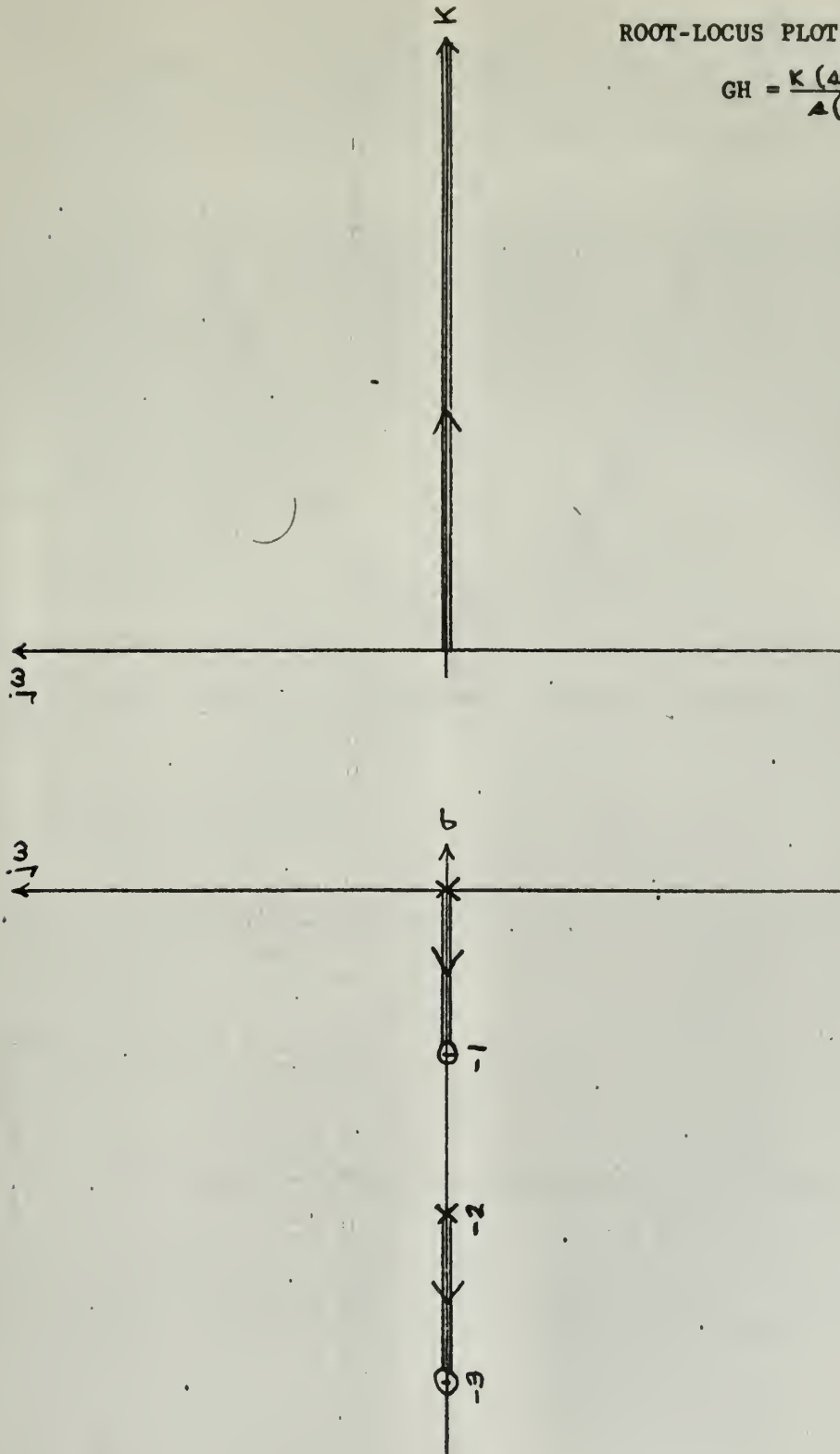ROOT-LOCUS PLOT AND K- $j\omega$ TRACE,

$$GH = \frac{K(s+1)(s+3)}{s(s+2)}$$

Fig. 2.2

22

ROOT-LOCUS PLOT AND K- $j\omega$ TRACE,

$$GH = \frac{K}{(\Delta+1)(\Delta+2)}$$
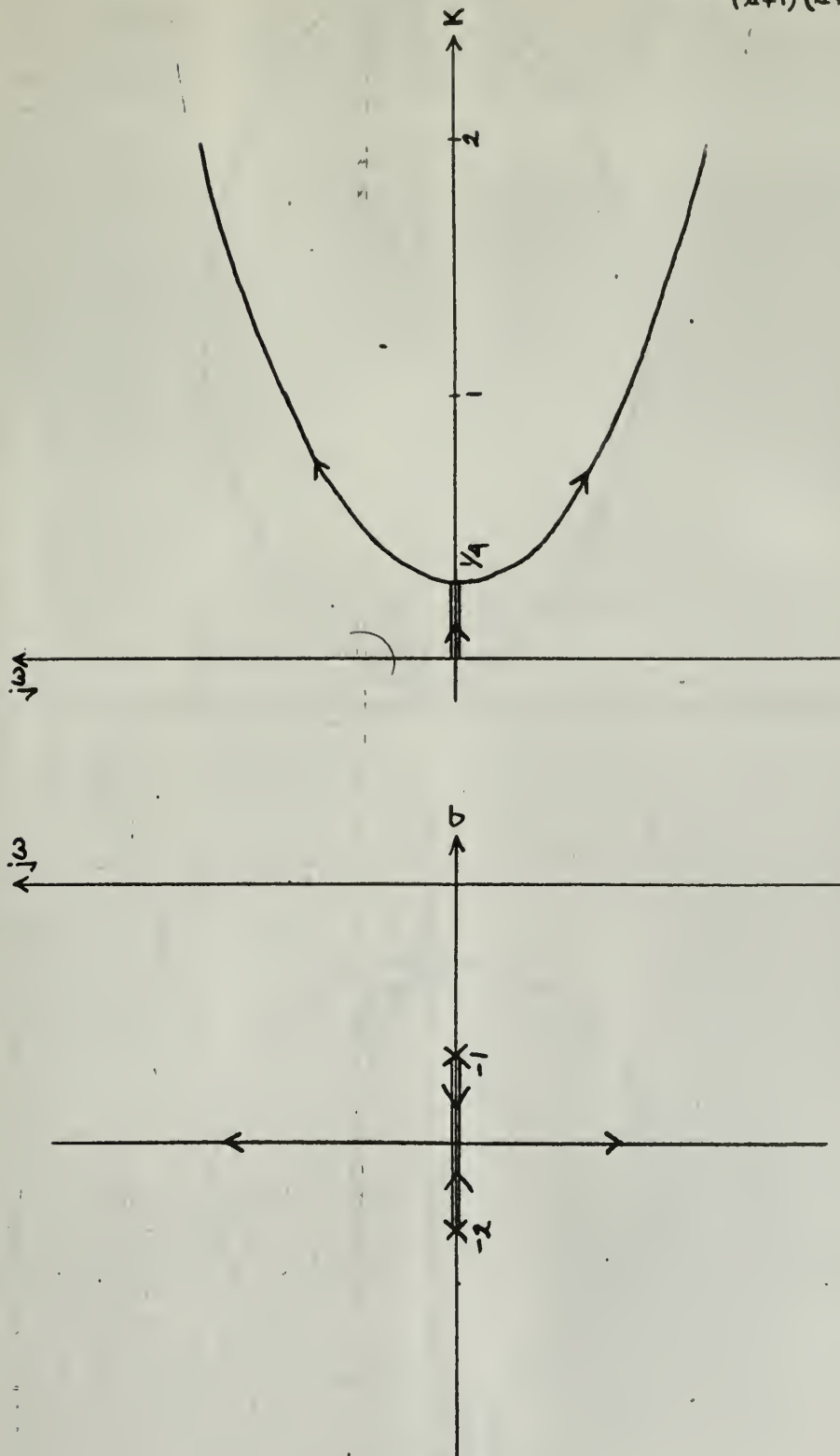
Fig: 2.3

23

ROOT-LOCUS PLOT AND K-$j\omega$ TRACE,
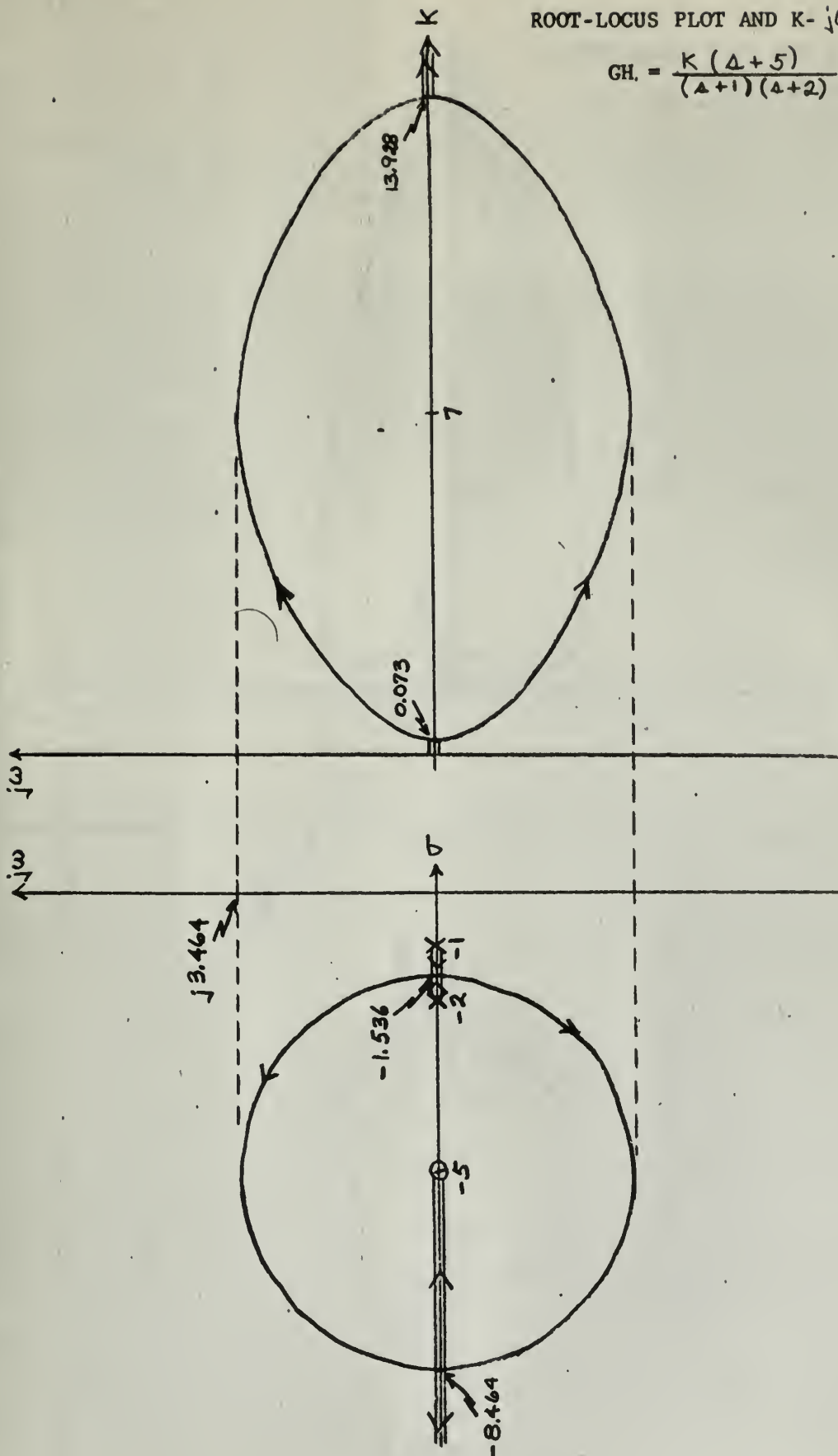
$$GH. = \frac{K(\Delta+5)}{(\Delta+1)(\Delta+2)}$$

Fig. 2.4

ROOT-LOCUS PLOT AND K-$j\omega$ TRACE,

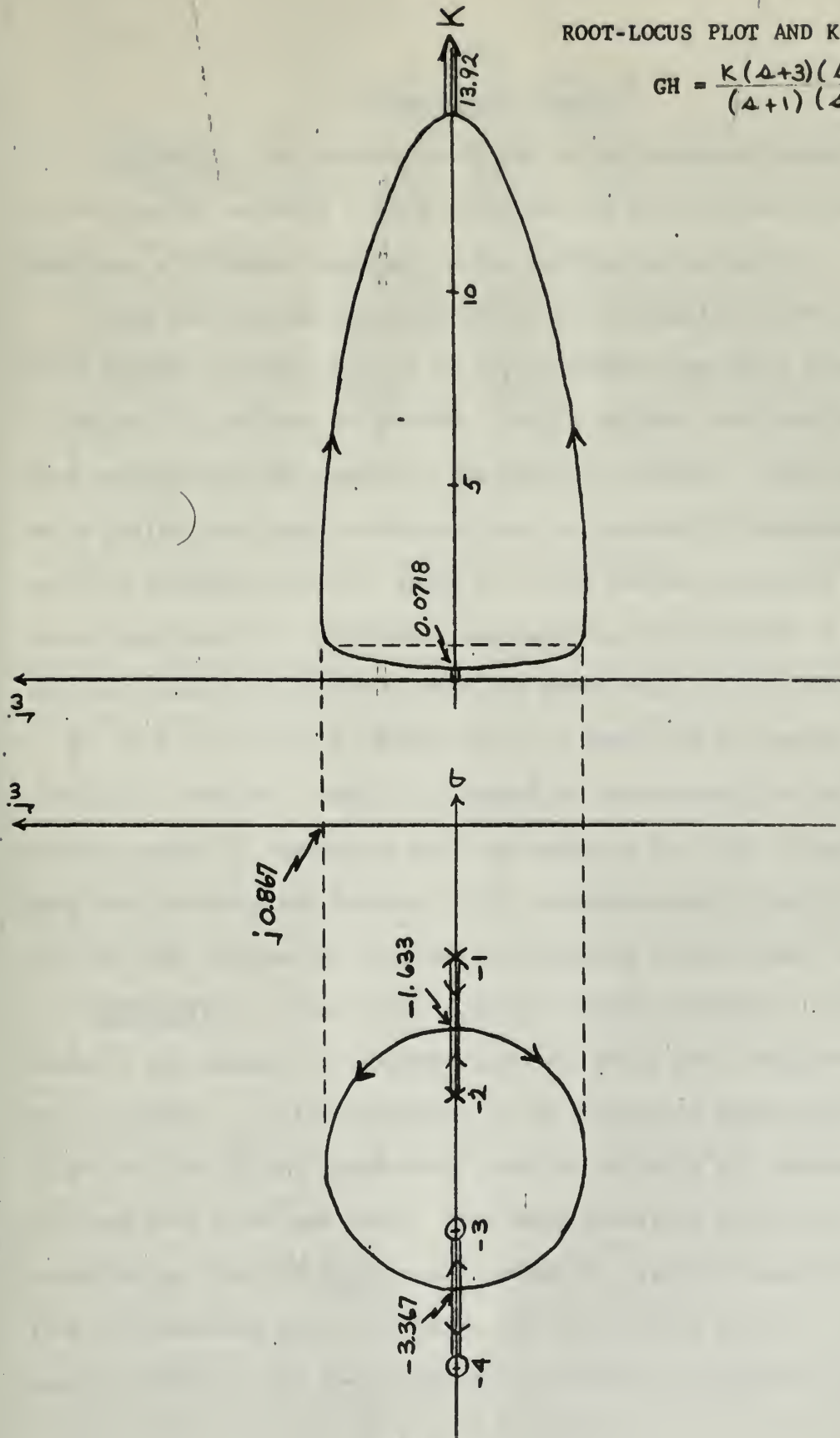$$GH = \frac{K(\Delta+3)(\Delta+4)}{(\Delta+1)(\Delta+2)}$$

Fig. 2.5

HIGHER-ORDER SYSTEMS

3.1. <u>PROCEDURE</u>. The methods developed in the previous chapter could not be readily extended to give solutions for higher order systems. Therefore a different approach to the problem was indicated.

Since the desired procedure was to be an addition to the root-locus method it seemed logical to try to extend root-locus techniques to achieve the desired projection. On the s-plane, the root-locus must satisfy both the magnitude and angle criterions. Those points which satisfy the angle requirement can be accurately determined by use of a Spi-rule, but this would be a very tedious procedure if other guide lines were not available. In practice, the centroid is computed and the asymptotes are drawn, then the root-locus can be rapidly "rough-ed in" with the Spi-rule used mainly as a check and to provide added accuracy if desired. Thus, if a method of determining the centroid and the angles of asymptotes could be found in the $K-j\omega$ plane, per-haps with practice the desired $K-j\omega$ projection could also be "roughed in" and then checked for accuracy as necessary by some other means.

3.2 <u>ASYMPTOTES</u>. To develop a method of finding asymptotes in the $K-j\omega$ plane it was helpful to consider first why there were asymptotes in the $\sigma-j\omega$ plane. As the parameter, K, is allowed to become very large, those roots which are approaching zeros at infinity are distant from the open loop poles and zeros. The angle condition must be met by the contribution from the <u>excess</u> poles since the algebraic sum of the angles from the remaining poles and zeros will effectively cancel. Thus, as K goes to infinity, the root locations allowable are limited to lying on

asymptotes having angles which, when multiplied by the number of excess poles, satisfy the angle criterion. The angle of the asymptote must be measured at the effective center or centroid of the open loop poles.

In much the same manner the value of gain required for a point on the s-plane asymptote which is distant from the open loop poles and zeros is determined by the product of the distances from that point to the excess poles, since the distances from the other poles and zeros will effectively cancel. An approximation for the gain at this point is the distance to the system centroid raised to the power n, where n is the number of excess poles. Referring to Fig. 3.1, the distance from a point, R, on the s-plane asymptote to the centroid is

$$d = \frac{\omega_1}{\sin \alpha}$$

where ω_1 is the value of ω at R_1 and α is the s-plane asymptote angle. Thus the magnitude of the gain is given approximately by

$$|K| \approx \left[\frac{\omega_1}{\sin \alpha} \right]^n \qquad \qquad 3.1$$

the approximation being valid if ω_1 is very large. Consequently, solving equation 3.1 for ω_1 and assuming ω_1 very large gave

$$\omega = (\sin \alpha) \sqrt[n]{|K|} \qquad \qquad 3.2$$

where α = the angle of the s-plane asymptote, and n = the number of excess poles. Equation 3.2 was obviously not linear in K and ω, implying the asymptotes in the s-plane did not transfer into straight line asymptotes in the K-$j\omega$ plane under the approximation used. This implication appeared to be a serious drawback to this method, because curved asymptotes could not, in general, be quickly and easily plotted. However, a compromise solution was reached: by letting the

27

$$\sin \alpha = \frac{\omega}{p}$$

$$p = \frac{\omega}{\sin \alpha}$$

Fig. 3.1

28
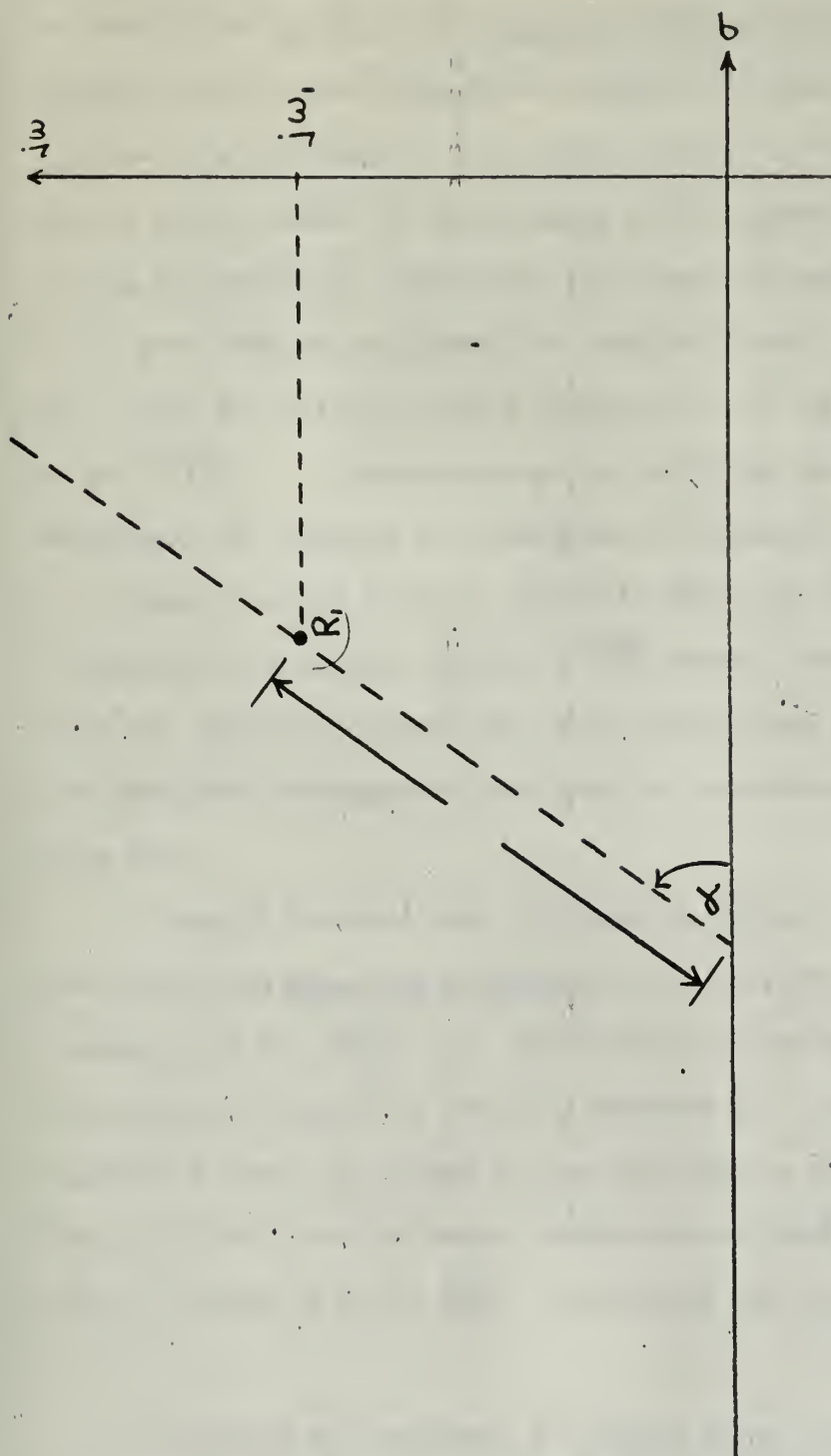
gain variable be $\sqrt[n]{|K|}$, equation 3.2 _is_ the equation of a straight line, since $\sin \alpha$ is a constant[1] for any given asymptote. Further, this straight line, _which is the s-plane asymptote transferred into the_ $\sqrt[n]{|K|} - j\omega$ _plane_, always passes through the origin with slope $= \sin \alpha$. Consequently, the only knowledge of the system required to quickly plot the asymptotes is n, the number of excess poles of the system. The advantage of having straight-line asymptotes, then, made the adoption of the $\sqrt[n]{|K|} - j\omega$ plane advisable for obtaining the required trace. The term "K-$j\omega$ trace" will still be utilized in this discussion, but the abscissa is implied to be $\sqrt[n]{|K|}$. A discussion of the relative advantages and/or disadvantages of adopting this procedure is contained in section 3.5.

Since the root locus is symmetric about the real axis the K-$j\omega$ trace will be symmetric about the $\sqrt[n]{|K|}$ axis. Thus, as in the root locus, only the upper or positive $j\omega$- axis need be used since the asymptotes and trace for the negative half would be the mirror image of the positive half.

It should be noted that for negative values of K the root locus obeys the same _magnitude criterion_ as for positive K. Therefore the asymptote in the $\sqrt[n]{|K|} - j\omega$ plane will obey the same equation for both positive and negative K, that is, equation 3.2. Thus the trace for negative K could be plotted on the same axes as for the positive K trace, but for clarity the following convention was established: The positive trace is drawn on the $+\sqrt{|K|}$ coordinate and negative trace on the

---

[1] It should be noted that for higher order systems there will be n asymptotes on the s-plane, each of which will be defined by an angle α_n. There will be a K-$j\omega$ asymptote for each s-plane asymptote defined by equation 3.2 utilizing the appropriate α_n.

$-\sqrt[q]{|K|}$ axis, with the $j\omega$ -axis passing through the zero point of the abscissa. Care must be used in plotting the K-$j\omega$ asymptotes, because they are <u>not</u>, in general, equally spaced (in the angular sense) as are the s-plane asymptotes. The K-$j\omega$ asymptotes for positive K and those for negative K must be sketched separately, for the angles of the s-plane asymptotes are different for positive and negative values of K. This is shown graphically in Fig. 3.2.

---Positive K
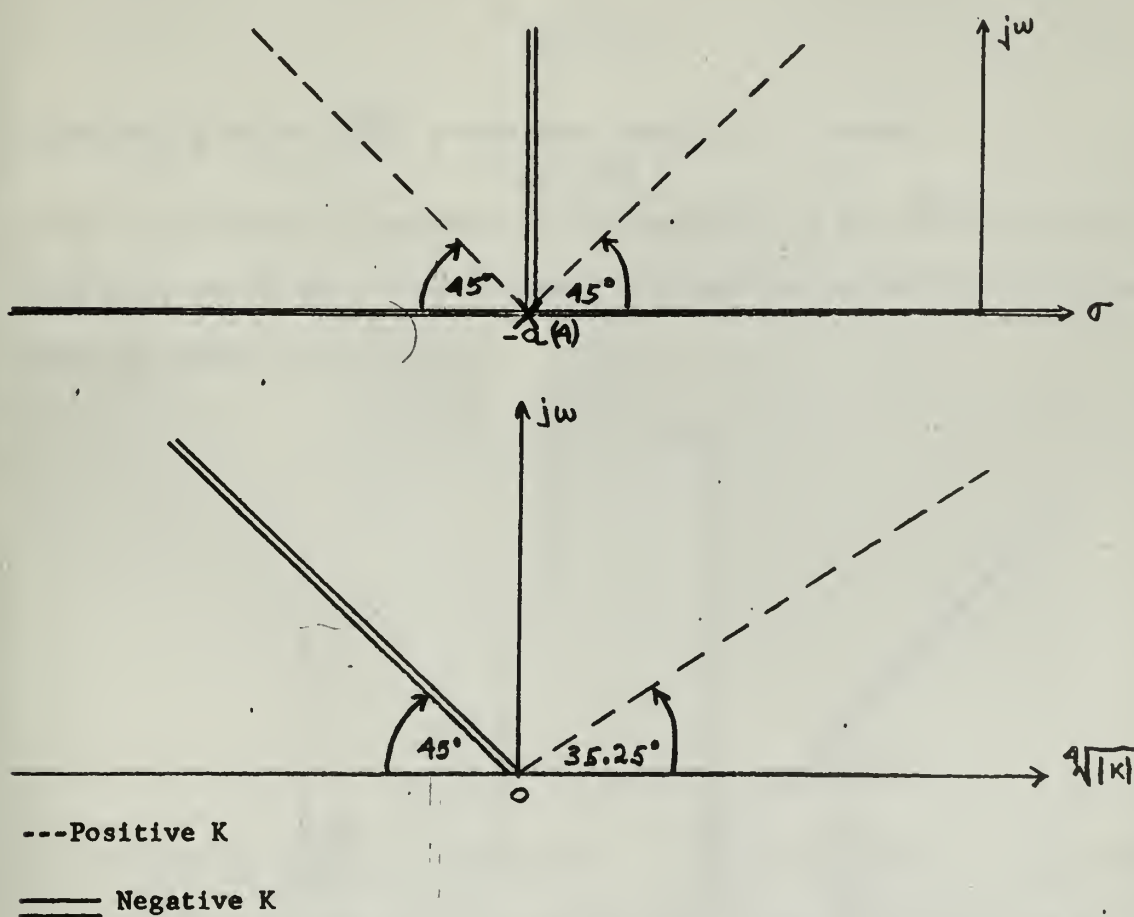
——— Negative K

ROOT LOCUS AND K-$j\omega$ ASYMPTOTES FOR GH = $\dfrac{K}{(s+a)^4}$ FOR POSITIVE AND NEGATIVE VALUES OF K , $j\omega \geq 0$.

Fig. 3.2

30

3.3 <u>K-jω TRACE</u>.   Having determined the asymptotes in the $\sqrt[2]{|K|}-j\omega$ plane, the first step in determining the K-jω trace involved a review of the procedures for sketching the K-jω trace of second-order systems as outlined in Tables 2.1 and 2.2.

As a first consideration, the real double pole/zero combination (as shown in category V of Table 2.1) produced no trace on the K-axis, and therefore had no trace on the $\sqrt{|K|}$ -axis, since the latter axis differed from the former only by a scale factor. Using Table 2.2 (for no zeros) and equation 2.10 yielded the equation

$$\omega^2 = K \qquad\qquad 3.3$$
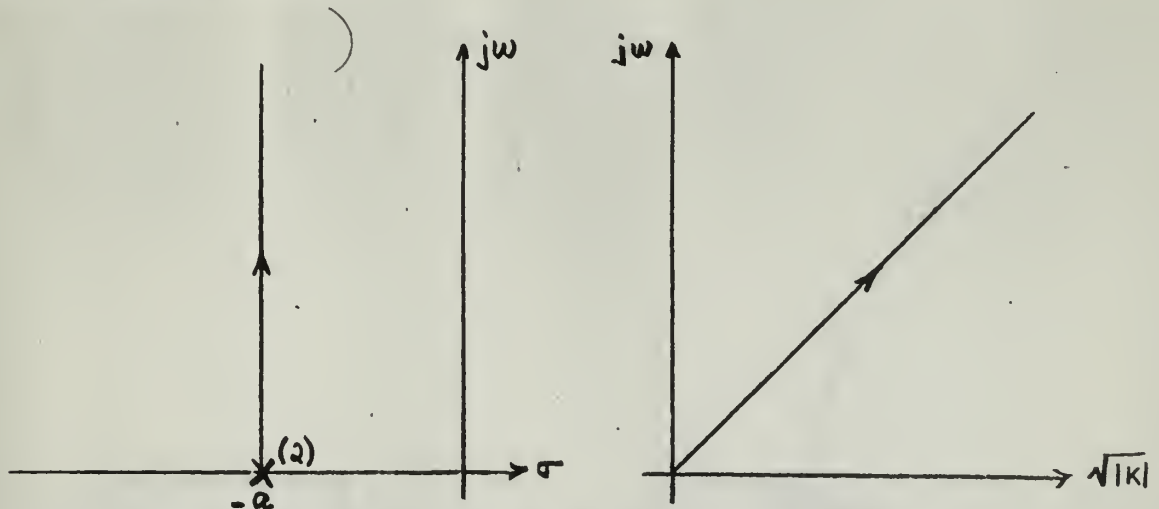
Transforming to the $\sqrt{|K|}$ coordinate, equation 3.3 became

$$\omega = \sqrt{K}$$

which is precisely the equation of the asymptote in the $\sqrt{|K|}-j\omega$ plane. Therefore, the K-jω trace for such a system lay entirely on the asymptotes, as shown in Fig. 3.3.
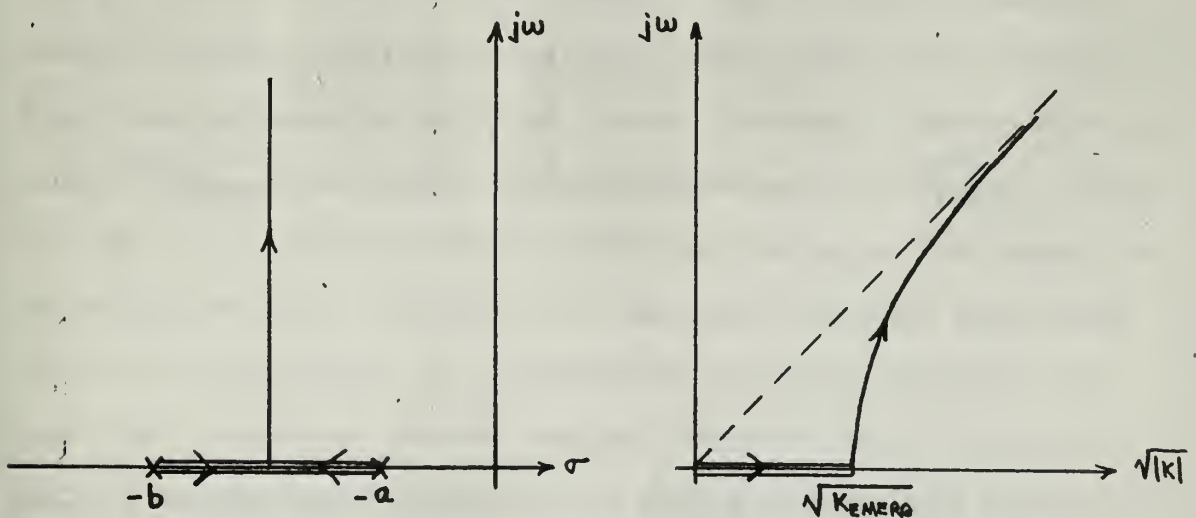

ROOT LOCUS PLOT AND K-jω TRACE FOR GH $= \dfrac{K}{(\Delta+a)^2}$, $K \gtrless 0$ AND $j\omega \gtrless 0$

Fig. 3.3

The extension to a real multiple pole of any order, then, was simply a combination of the foregoing result and successive applications of Table 2.1, resulting in the conclusion that a real multiple pole/multiple zero of any multiplicity will have a K-$j\omega$ trace which coincides precisely with the K-$j\omega$ asymptotes. For poles of odd multiplicity, of course, the entire $\sqrt[n]{|K|}$ -axis will be part of the trace, since the odd pole falls under category I in Table 2.1.

As the poles of a real double pole combination are separated along the σ -axis, the change in the K-$j\omega$ trace (from that obtained for the double pole) was expected to be most noticeable near the origin, since the curve must become asymptotic for increasing values of K. Further, the value of K at which the trace departs the K-axis has already been determined to be K_{EMERG} (which becomes $\sqrt{K_{EMERG}}$ on the $\sqrt{K}$ -axis). Consequently, the K-$j\omega$ trace was sketched as shown in Fig. 3.4.

ROOT LOCUS PLOT AND K-$j\omega$ TRACE FOR GH = $\frac{K}{(4+a)(4+b)}$, $K \geq 0$ AND $j\omega \geq 0$

Fig. 3.4.

For this special case, i.e., an open-loop transfer function $GH = \frac{K}{(\Delta+a)(\Delta+b)}$, an interesting property of the K-$j\omega$ trace became apparent. The K-$j\omega$ trace in Fig. 3.4 bore a striking resemblence to the root locus plot of $GH = \frac{K}{(\Delta+a)^2(\Delta+b)^2}$, as may be seen by comparing Fig. 3.4 with Fig. 3.5, if the pole, a, was related to $\sqrt{K_{EMERG}}$.
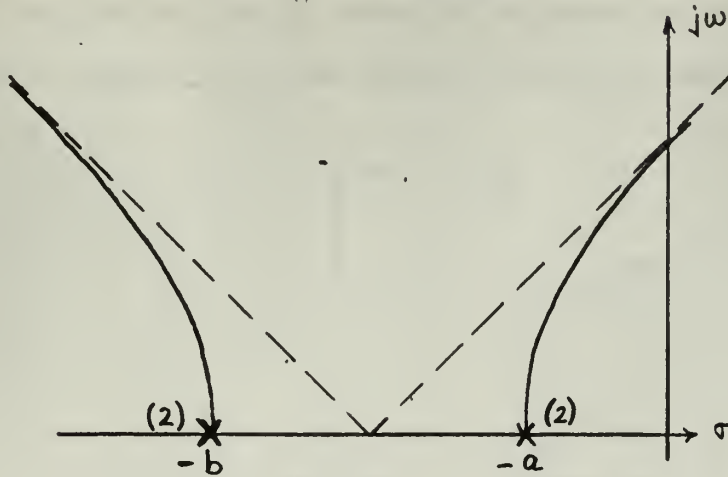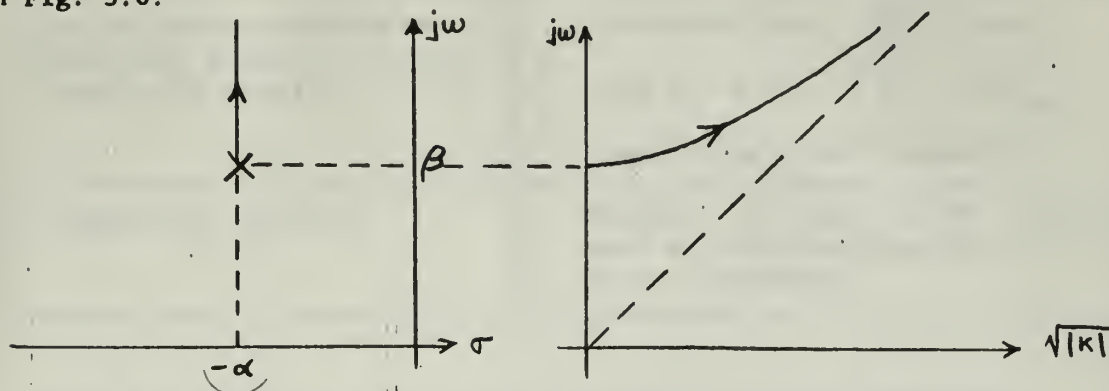

ROOT LOCUS PLOT FOR $GH = \frac{K}{(\Delta+a)^2(\Delta+b)^2}$, $K \geq 0$ AND $j\omega \geq 0$

Fig. 3.5

Since all points on the root locus shown in Fig. 3.5 must necessarily satisfy the angle criterion, it was felt that a similar angle criterion might be established for the K-$j\omega$ trace. Locating a simulated double pole at $\sqrt[2]{K_{EMERG}}$ and another simulated double pole at $-\sqrt{K_{EMERG}}$ in Fig. 3.4, the K-$j\omega$ trace satisfied a 180° angle criterion with respect to these simulated poles - precisely the same angle criterion established for the root locus plot! It was concluded, therefore, that the K-$j\omega$ trace for an open-loop transfer function consisting of two real poles could be sketched quickly and could be checked directly with a Spi-rule (utilizing the simulated poles described earlier) if greater accuracy was required.

33

For an open-loop transfer function consisting of a pair of complex poles, the K-$j\omega$ trace was easier to sketch than for any other pole-zero configuration. Since the $j\omega$-axis was common to both the root locus plot and the K-$j\omega$ trace, and since the trace must be asymptotic, it was a simple matter to sketch the trace departing the $j\omega$-axis at the complex values of the poles and approaching the 45° asymptote. The K-$j\omega$ trace for such a pair of complex poles is shown in Fig. 3.6.

ROOT LOCUS PLOT AND K-$j\omega$ TRACE FOR GH = $\dfrac{k}{[\Delta+(\alpha+j\beta)]\,[\Delta+(\alpha-j\beta)]}$,
$K \geq 0$ AND $j\omega \geq 0$

Fig. 3.6

The procedures to use in sketching the K-$j\omega$ traces for the foregoing "basic pole configurations" of an open-loop transfer function are summarized in Table 3.1. These procedures are equally applicable by replacing the word "pole" by the word "zero", " $\sqrt{K_{EMERG}}$ " by " $\sqrt{K_{ENT}}$ ", and "K = 0" by "K = infinity" where they appear in Table 3.1. Thus, Table 3.1 is applicable to both basic pole and basic zero configurations.

Only one more general type of response remained to complete the procedures for obtaining the K-$j\omega$ trace for any given open-loop transfer function: namely, the influence upon the trace of poles and zeros contained in the transfer function in addition to the basic combinations already discussed. The influence of these additional poles and zeros

34

BASIC POLE CONFIGURATION	K- $j\omega$ TRACE

I. Multiple (real) pole.	1. Even multiplicity:
	
	   a. Trace coincident with asymptotes for all $j\omega$.
	
	2. Odd multiplicity:
	
	   a. Trace coincident with asymptotes for $j\omega \neq 0$.
	
	   b. Trace coincident with $\sqrt[n]{|K|}$ -axis for $j\omega = 0$.

II. Real pole-pole combination (with root locus on σ -axis between the poles).	Coincident with $\sqrt[n]{|K|}$ -axis from K = 0 to $\sqrt{K} = \sqrt{K_{EMERG}}$. then rising toward asymptote.
III. Complex pair of poles.	Departs $j\omega$ -axis at $j\omega$ = complex part of pole, approaches the K- $j\omega$ asymptote.

RULES FOR SHAPE OF K- $j\omega$ TRACE FOR BASIC POLE CONFIGURATIONS
OF OPEN-LOOP TRANSFER FUNCTION
Table 3.1

was most apparent graphically by returning to the multiple pole concept.

Starting with a real pole of multiplicity three, the influence upon the

K- $j\omega$ trace of moving <u>one</u> of these three poles along the σ -axis

while keeping the other two poles fixed was to cause the trace to "sag"

below the trace obtained for the triple pole. This is shown in Fig. 3.7.

It was possible to predict the sag intuitively by considering the graphi-

cal definition of K. Since K is defined (graphically) as the product of

the distances to poles divided by the product of the distances to zeros,

it was immediately obvious that, for a given value of $j\omega$ in the lower

range where the root locus of Fig. 3.7(b) was distinctly separate from

the asymptote, the value of K must be larger than the value in Fig. 3.7(a).
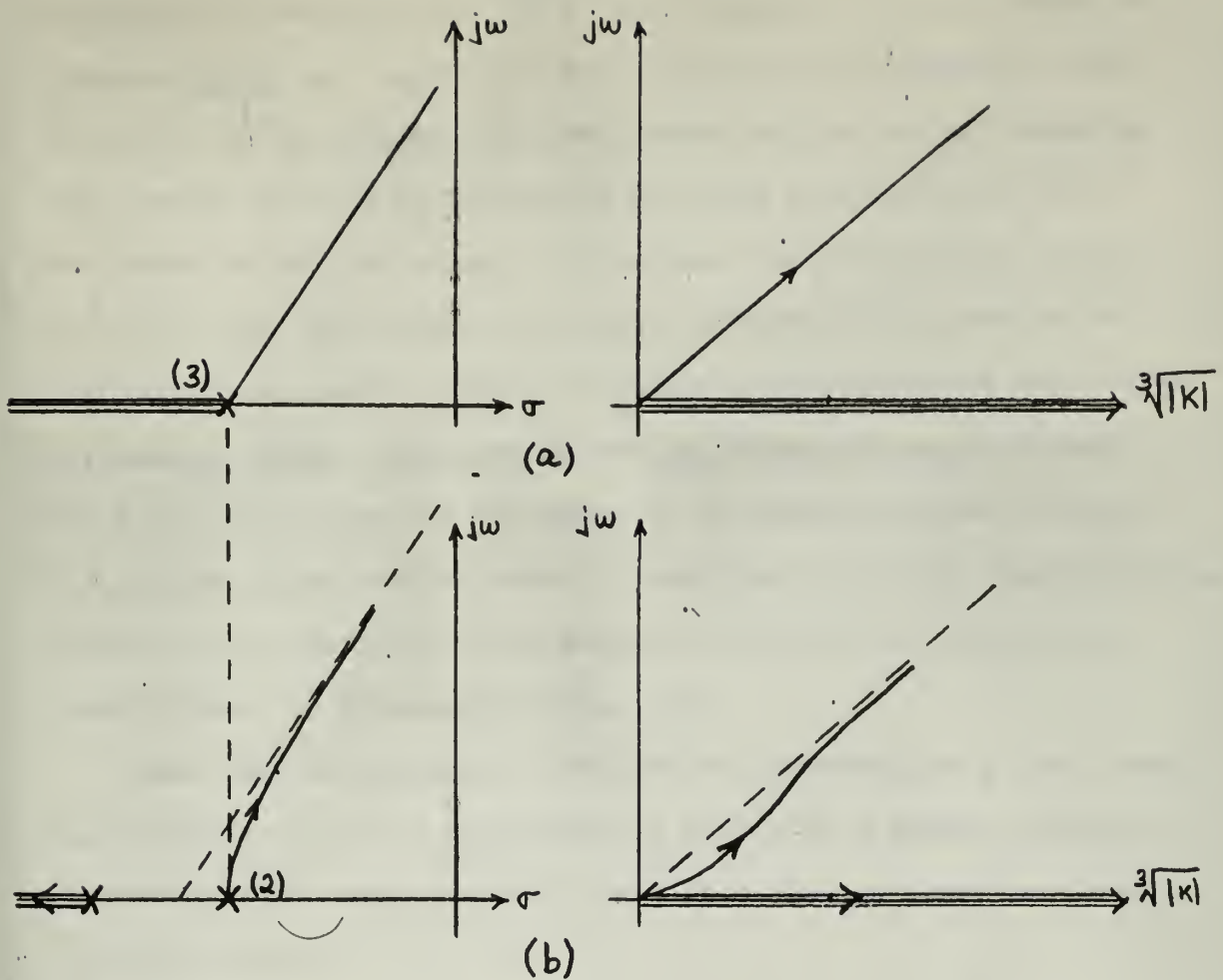
"SAG" EFFECT OF ADDITIONAL POLE UPON K- $j\omega$ TRACE
Fig. 3.7

Consequently, the sag was anticipated. In addition, as K was increased

to larger values, the poles of Fig. 3.7(b) would appear closer together

from the point on the root locus where K was measured until, in the limit

as K approached infinity, the poles would appear as a triple pole. This,

then, caused the asymptotic return of the K- $j\omega$ trace after the sag ef-

fect.

The effect of zeros upon the K- $j\omega$ trace was obtained in a similar

manner, but in order to show the effect upon a single diagram, the number

of excess poles, n, of the open-loop transfer function had to remain

unchanged in order that the $\sqrt[n]{|K|}$ -axis remained the same. Therefore pole-zero pairs were added. By again considering the graphical definition of K, it was apparent that two effects would be evident depending upon whether the pole or the zero of the added pair was closer to a test point on the root locus. For the case where the zero was closer to the root locus, the distance to the pole exceeded the distance to the zero, resulting in an overall value of K which was larger than the value before the pair was added. Consequently, the sag effect was again produced. Where the pole of the pair was closer to the root-locus than the zero, the reverse effect resulted due to a reduction in K, which caused the K-$j\omega$ trace to "rise" above the trace obtained without the pole-zero pair. These effects are illustrated in Fig. 3.8.

Based upon the procedures developed for sketching the K-$j\omega$ trace, the following rules were established to be used as a general procedure to be followed in obtaining the K-$j\omega$ trace for any given open-loop transfer function:

1. Sketch the root locus plot for the open-loop system.

2. Group the poles of the transfer function into the basic configurations listed in Table 3.1. Poles and zeros left over after this basic grouping is performed are designated in pairs as "additional pole-zero pairs".

3. Poles left over after the pairing operation described above are paired together (if there is root locus on the σ-axis between them) and designated as "pole-pole combinations".

4. Any real pole remaining is designated as an "unpaired

37

$$GH = \frac{K(\Delta+c)}{(\Delta+a)^2(\Delta+b)(\Delta+d)}$$

(a)
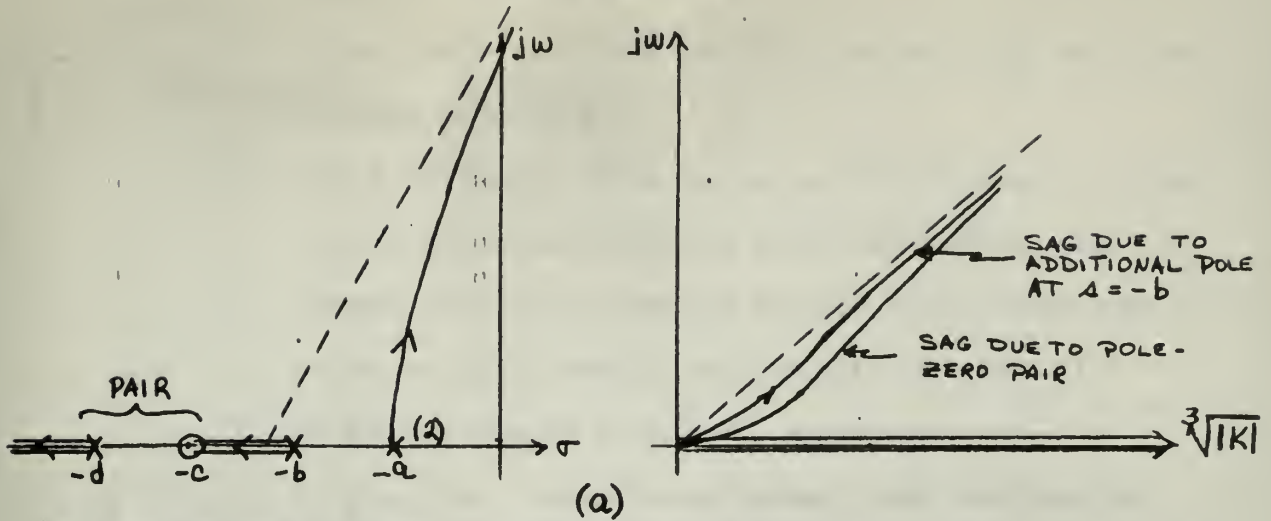
SAG EFFECTS DUE TO ADDITIONAL POLE AND POLE-ZERO PAIR, $K \gtrless 0$ AND $j\omega \geq 0$

$$GH = \frac{K(\Delta+d)}{(\Delta+a)^2(\Delta+b)(\Delta+c)}$$

(b)
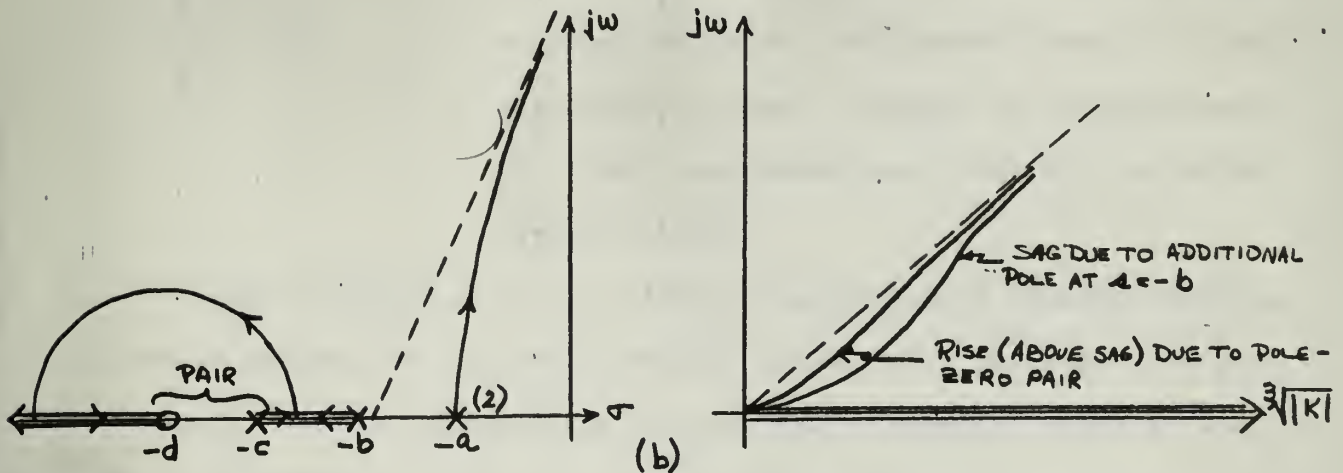
RISE EFFECT DUE TO POLE-ZERO PAIR (PORTION OF K- $j\omega$ TRACE DUE TO CIRCULAR ROOT LOCUS NOT SHOWN)

SAG AND RISE EFFECTS DUE TO ADDITIONAL POLES AND POLE-ZERO PAIRS

Fig. 3.8

38

pole".[1]

5. Sketch the K- $j\omega$ trace for $\omega = 0$ by utilizing the rules outlined in Table 2.1.

6. Sketch the K- $j\omega$ trace for $\omega \neq 0$ for all basic pole configurations by utilizing the rules outlined in Table 3.1.

7. Correct for the rise and sag effects of all additional pole-zero pairs (and an unpaired pole, if present).

8. To achieve greater accuracy if required:

   a. For a second-order system, apply the rules of chapter II to obtain an exact K- $j\omega$ trace.

   b. For higher-order systems, measure the distances to poles and zeros from a few selected points on the root locus, then calculate K to achieve greater accuracy within any questionable range of K. This procedure is closely analagous to the refinement of a root locus sketch with a Spi-rule to achieve greater accuracy.

With practice, the K- $j\omega$ trace for _any_ open-loop transfer function can be rapidly and accurately sketched utilizing the rules set down previously. Several examples for certain types of transfer functions are

---

[1]
Steps 3 and 4 may result in zero-zero combinations and an unpaired zero if the open-loop transfer function should contain more zeros than poles. By the same token, step 2 could result in multiple real zeros. However, these eventualities are rare enough in engineering practice that they are not specifically mentioned in these rules. Should these situations be encountered, all the procedures developed for poles are equally applicable to zeros and may be applied in either case.

illustrated in section 3.4.

3.4 **EXAMPLES.** The following examples were chosen to illustrate the procedures developed for sketching the K- $j\omega$ trace:

1. $GH = \dfrac{K}{(\lambda+1)^2 (\lambda+3)}$

   a. The root locus for this system was sketched and is shown in Fig. 3.9.

   b. Since there are three poles the K- $j\omega$ trace must be on the $\sqrt[3]{K}$- $j\omega$ coordinates.

   c. The asymptote on the $\sqrt[3]{K}$- $j\omega$ plane will have a slope equal to sin 60° or 0.866.

   d. The open loop transfer function is composed of a double real pole and an "unpaired" pole so that the K-trace would be expected to originate at the origin and sag below the asymptote due to the "unpaired" pole. The resulting K- $j\omega$ trace is shown in Fig. 3.10.

   e. To verify the accuracy of the sketch, the gain required at ω equal to one was determined from the root locus to be equal to 2.55. From the K- $j\omega$ trace at ω equal one, $\sqrt[3]{K} = 1.38$, or K = 2.62.

2. $GH = \dfrac{K(\lambda+4)}{(\lambda+1)^2 (\lambda+3)(\lambda+5)}$

   a. The root locus was sketched as in Fig. 3.11.

   b. The open loop transfer function contains a double pole, an "additional pole-zero pair" and an "unpaired" pole. Thus for $j\omega \searrow 0$, the trace will originate at the origin and will sag below the asymptote due to both the "unpaired" pole and the "additional unpaired pole-zero pair". The effect of the pole-zero pair, $\dfrac{\lambda+4}{\lambda+5}$, will be to increase

40

the gain required to obtain a particular value of ω ,
since the zero is nearer to the test point than the pole.
Thus the K-$j\omega$ trace will have a larger sag than was
found in the previous example. The K-$j\omega$ trace is shown
in Fig. 3.12.

c. To check the accuracy of the K-$j\omega$ sketch, the gain
was compared at ω equal to one. From the root locus, K
was equal to 3.3. The K-$j\omega$ sketch gave $\sqrt[3]{K} = 1.49$,
or K = 3.31. At ω = 3.0 the root locus gain equalled 50
and the K-$j\omega$ trace gave $\sqrt[3]{K} = 3.67$ or K = 49.4.

3. $GH = \dfrac{K(s+1)}{(s+2)(s+3)^2(s+5)}$

a. The root locus is shown in Fig. 3.13.

b. As in example 2, the open loop transfer function is
composed of a double pole, an "unpaired" pole, and an
"additional pole-zero pair". In this case the "additional
pole-zero pair" is placed so that the pole is closer to
the test point than the zero, which tends to move the K-$j\omega$
trace upward-so far, in fact, that the trace actually
crosses the asymptote. This upward tendency will be partly
counteracted by the "unpaired" pole which will cause the
K-$j\omega$ trace to "sag" near the origin. The resulting K-$j\omega$
trace is shown in Fig. 3.14. It should be noted that the
effect of the "additional pole-zero pair" will change as ω
becomes greater than 4.4. Then, the pole will be farther
from the test point than the zero, which will tend to make
the trace sag, but this sag will be small since the test
point is quite distant from the open-loop poles and zero.

41

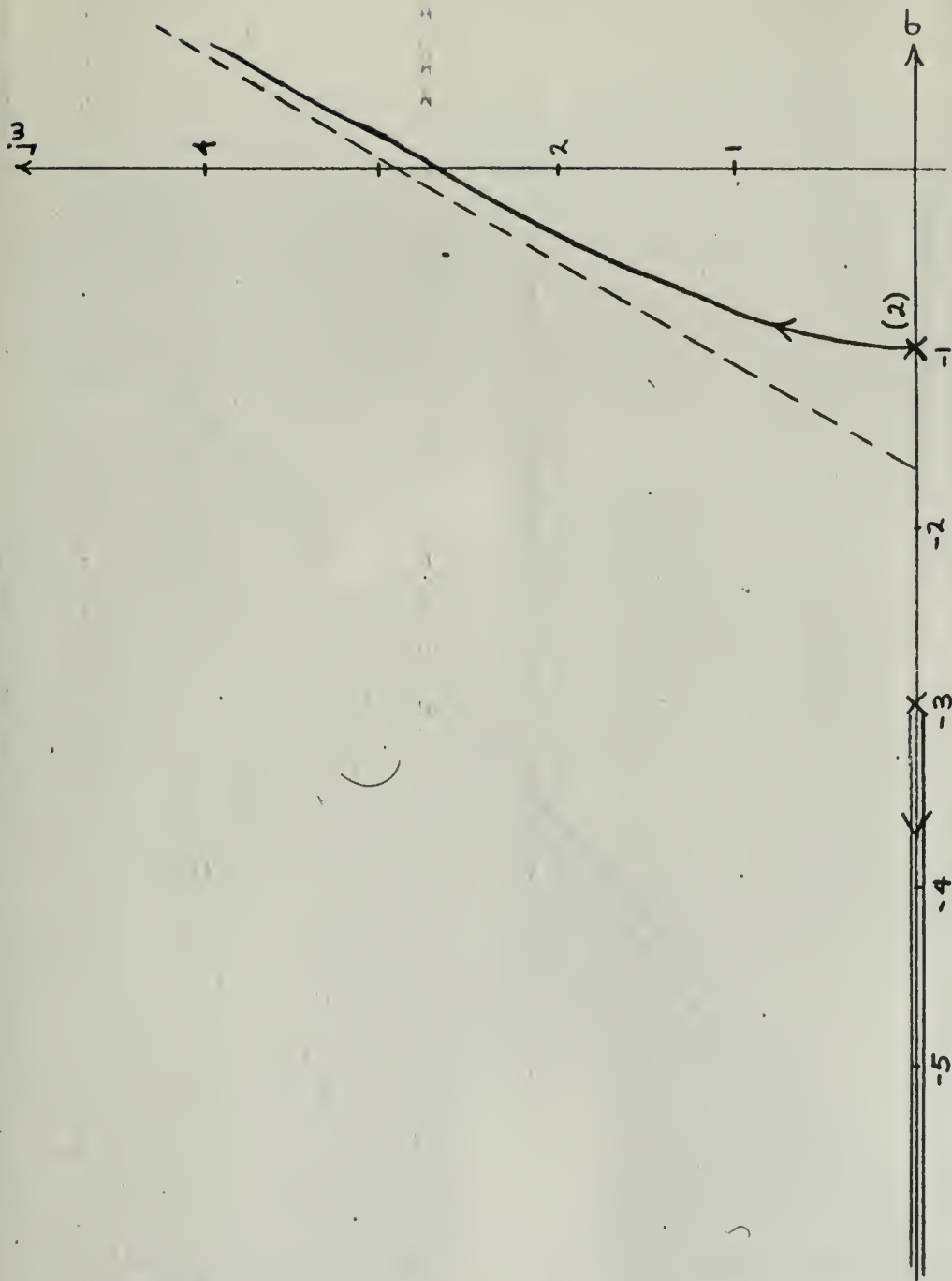ROOT LOCUS PLOT
FOR

$$GH = \frac{K}{(\Delta+1)^2 (\Delta+3)}$$

Fig. 3.9

42

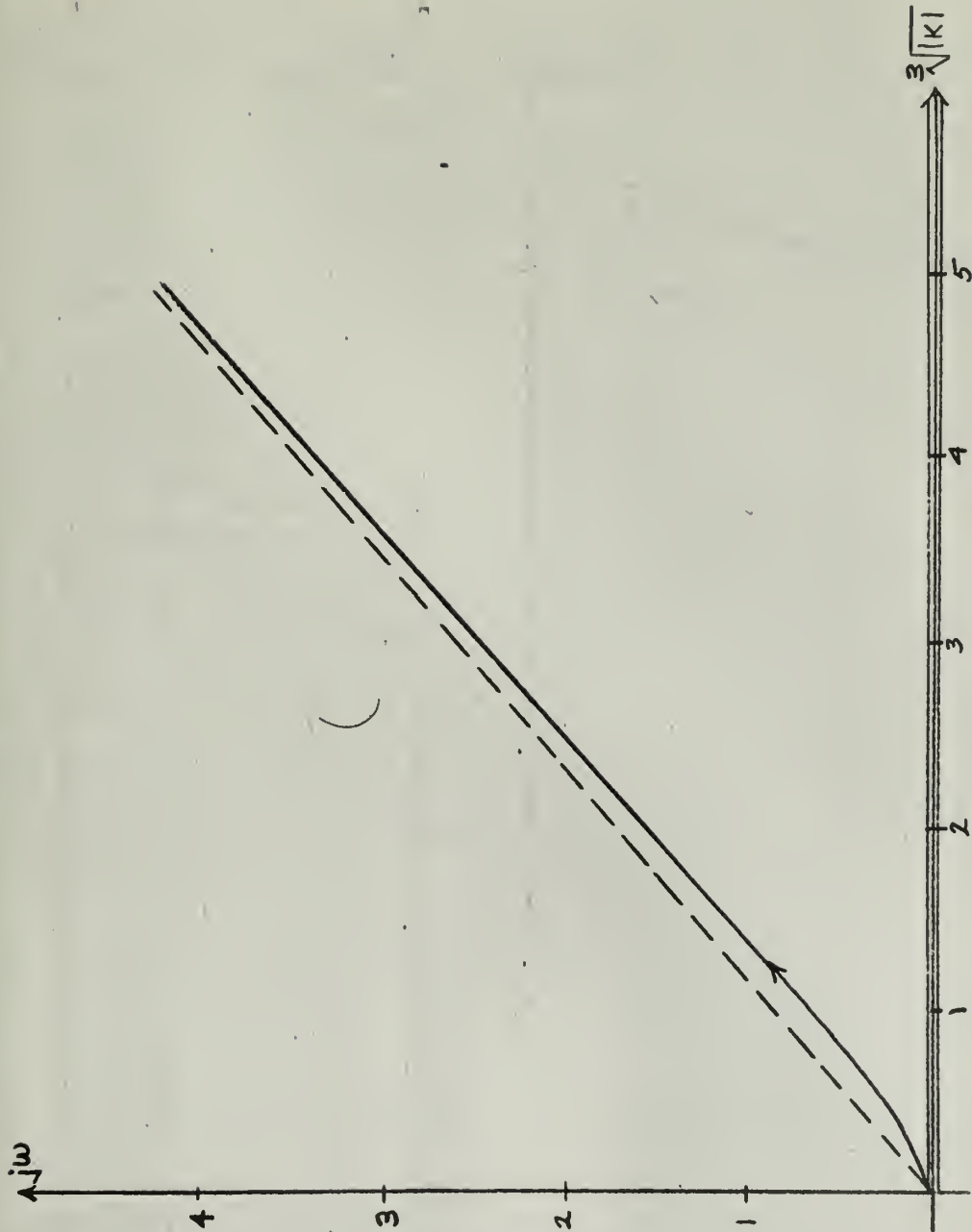K- $j\omega$ TRACE FOR

GH = $\dfrac{K}{(s+1)^2\,(s+3)}$

Fig. 3.10

43

ROOT LOCUS PLOT
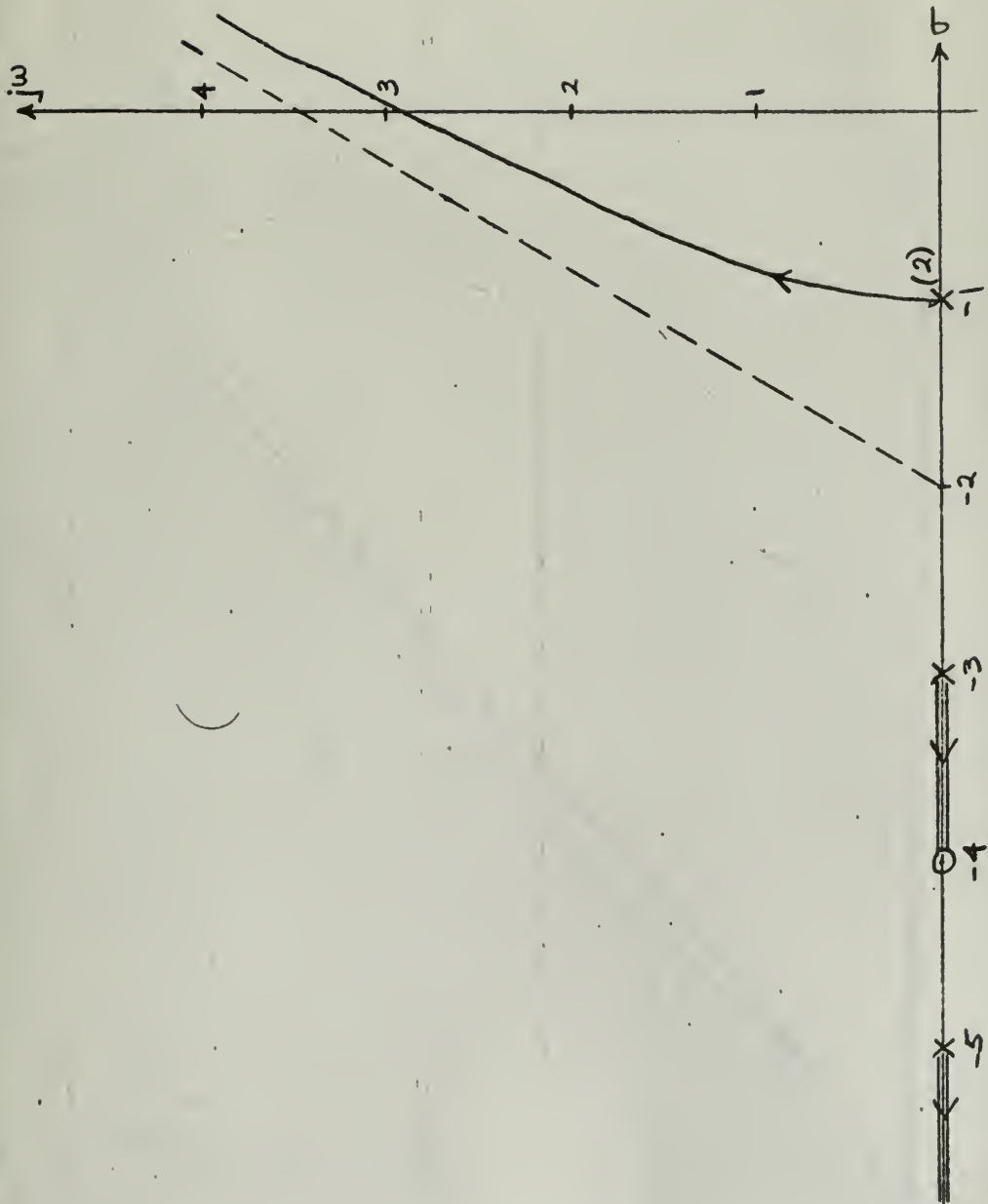FOR
$$GH = \frac{K(s+4)}{(s+1)^2(s+3)(s+5)}$$

Fig. 3.11

44

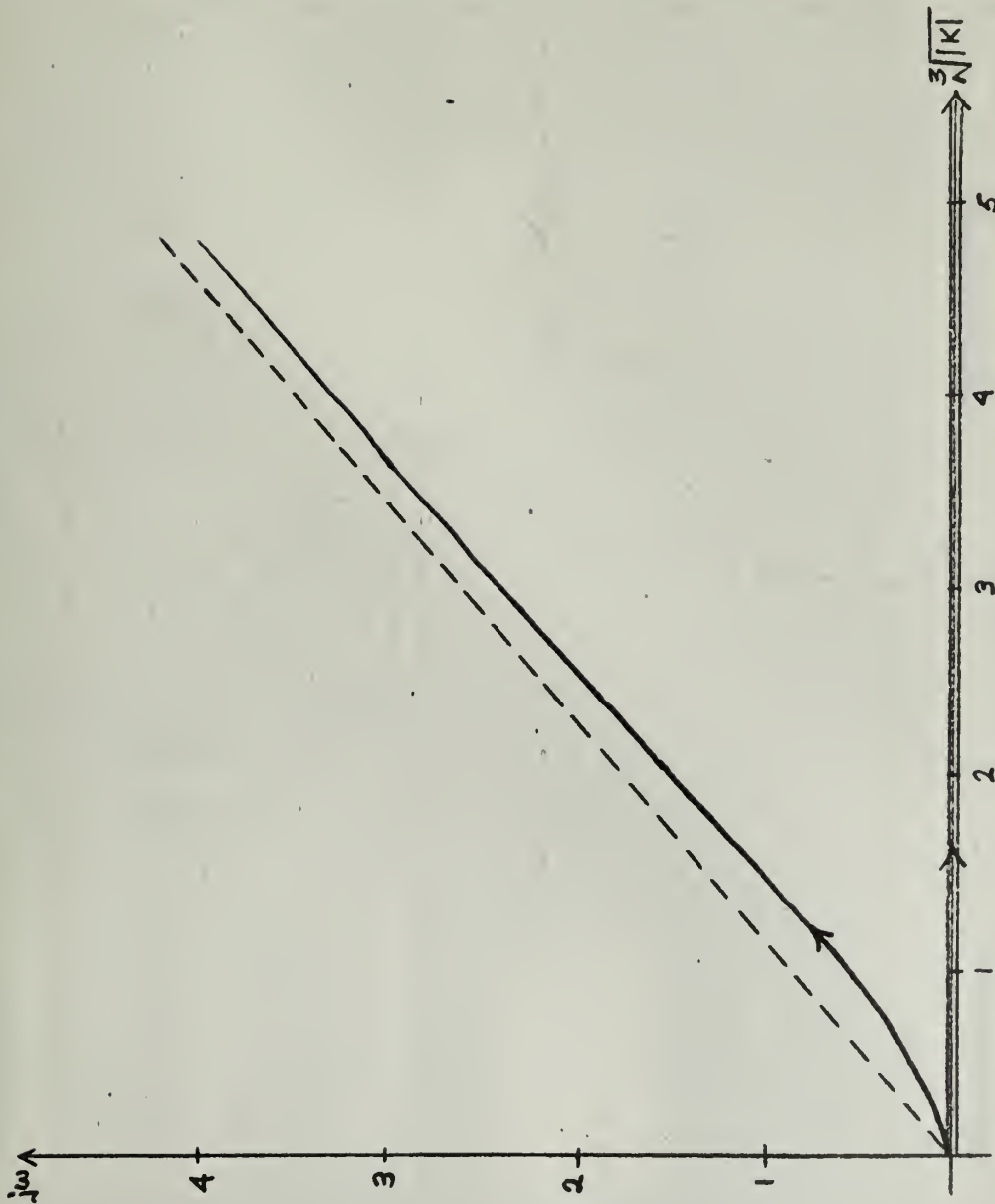K- jω TRACE FOR

$$GH = \frac{K(s+4)}{(s+1)^2(s+3)(s+5)}$$

Fig. 3.12

45

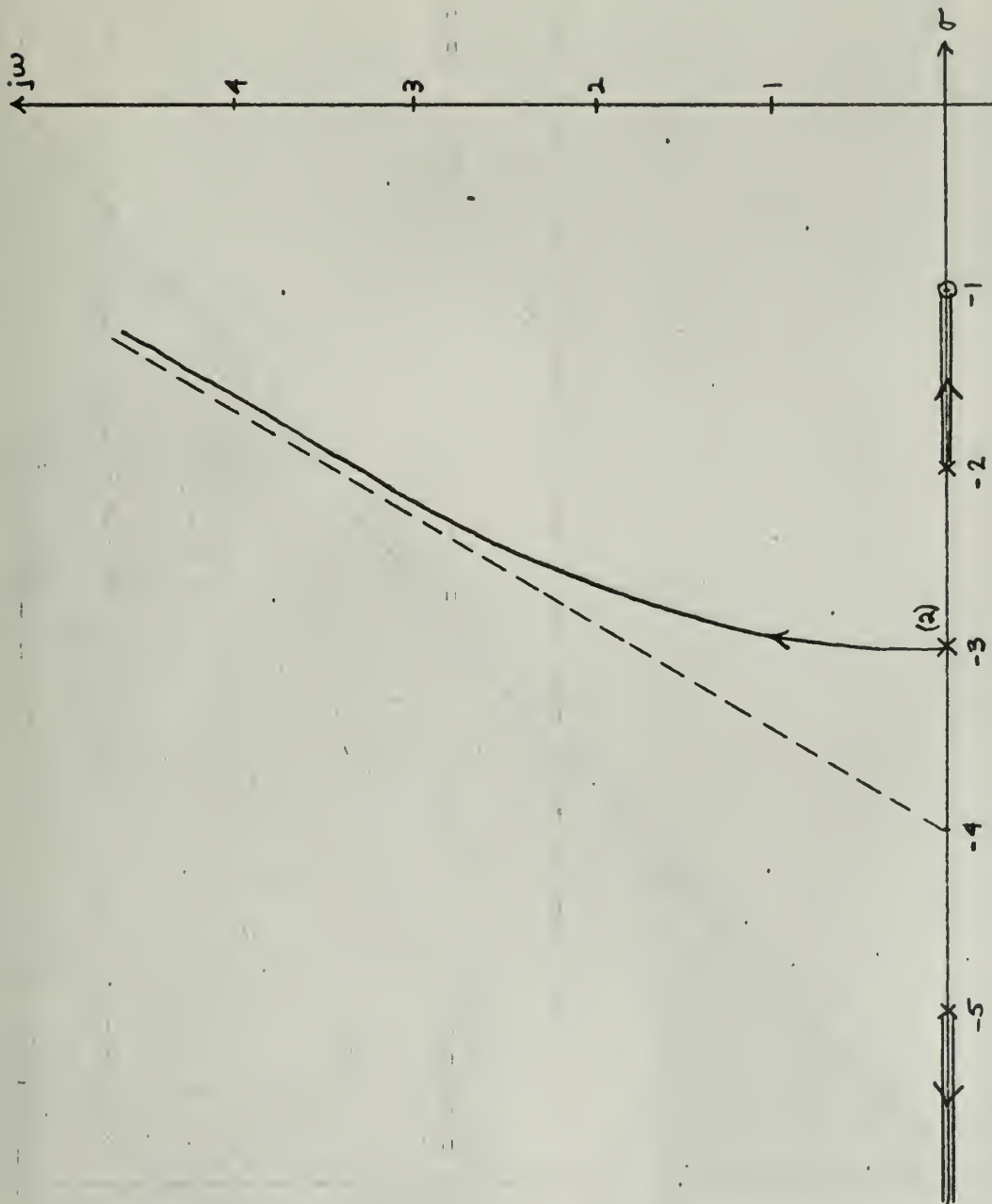ROOT LOCUS PLOT
FOR

$$GH = \frac{K(s+1)}{(s+2)(s+3)^2(s+5)}$$

Fig. 3.13

K- $j\omega$ TRACE FOR

$$GH = \frac{K(\Delta+1)}{(\Delta+2)(\Delta+3)^2(\Delta+5)}$$
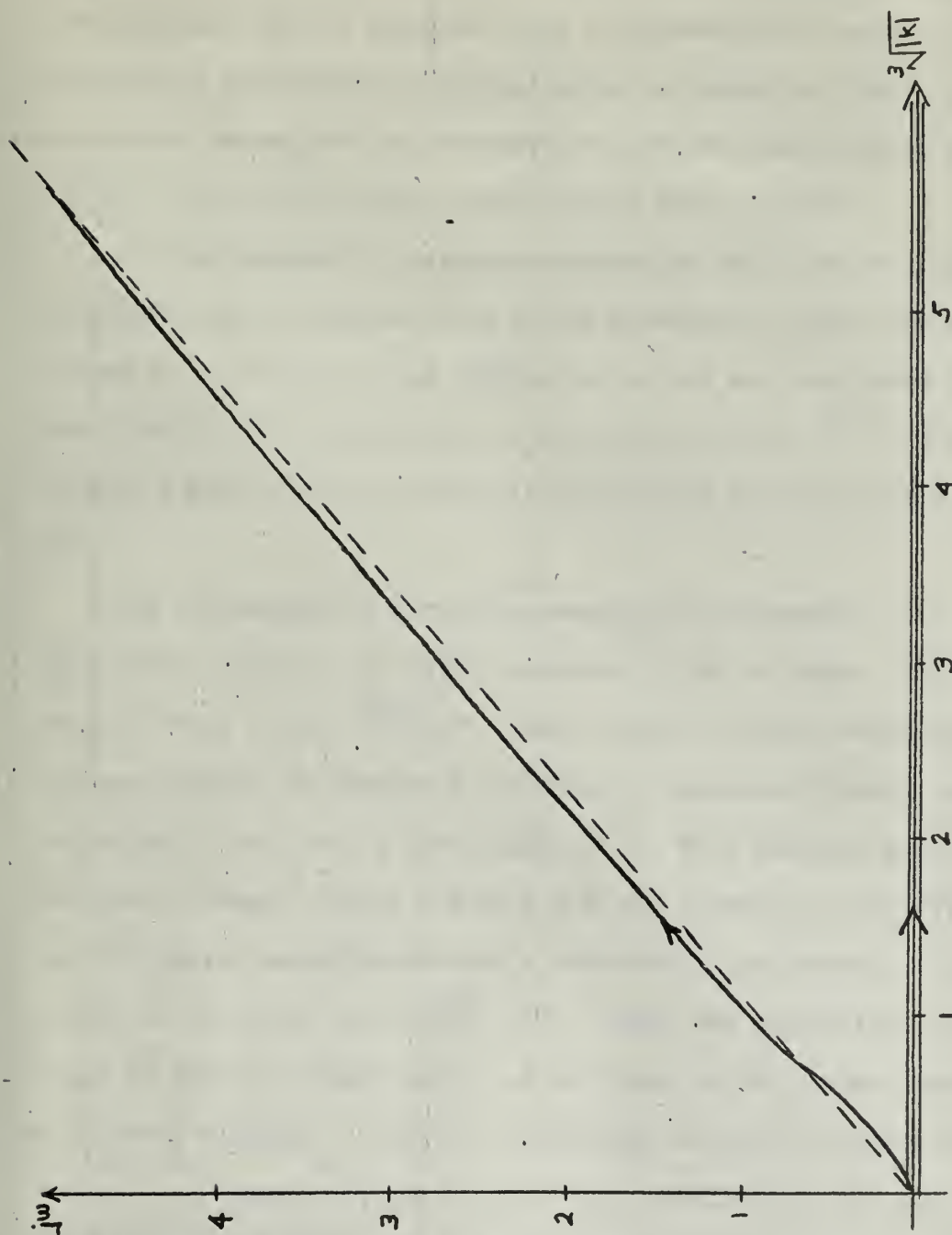

Fig. 3.14

This sag causes the asymptotic return of the trace to the upper side of the asymptote.

3.5 **INTERPRETATION OF K-$j\omega$ TRACE.** Having attained the initial objective of determining the K-$j\omega$ trace for any open-loop transfer function, the results remained to be interpreted with respect to the reasons for performing the determination as stated in chapter I. The difficulty anticipated in interpretation of the trace was the use of the $\sqrt[n]{|K|}$ abscissa for third (and higher) order systems.

For the purpose of obtaining information about the position of the imaginary part of complex roots of the closed-loop system for particular values of K, the use of the $\sqrt[n]{|K|}$ abscissa was not considered to be objectionable. This information is available from the $\sqrt[n]{|K|}-j\omega$ coordinates with a simple slide-rule calculation for any desired value of K.

For the purpose of obtaining sensitivity information over a given range of K, however, the $\sqrt[n]{|K|}$ abscissa is not so handy. The K-$j\omega$ trace plotted on the $\sqrt[n]{|K|}-j\omega$ plane can not be used conveniently to determine whether the frequency variation is constant, linear, exponential, asymptotic, etc., over a given range of K. This handicap may be easily overcome, however, due to the fact that the conversion from $\sqrt[n]{|K|}$ to $|K|$ can be readily accomplished with a slide-rule. By choosing a few key points on the trace in the $\sqrt[n]{|K|}-j\omega$ plane, the conversion to the K-$j\omega$ plane is readily accomplished, and the trace in the latter plane can be quickly sketched. Little is sacrificed in speed to obtain the additional information provided by the K-$j\omega$ coordinates, and the accuracy of the trace is still basically dependent upon the accuracy of the root locus plot. Speed of plotting must necessarily be inversely proportional

to the accuracy achieved, but the majority of the time is devoted to an accurate root locus plot and an accurate K- $j\omega$ trace in the $\sqrt[n]{|K|}$ $-j\omega$ plane - the conversion of the trace to the K- $j\omega$ plane would involve a negligible amount of time in comparison to that amount already spent in obtaining the first trace.

It was concluded, therefore, that the use of the $\sqrt[n]{|K|}$ abscissa does not present a material disadvantage to the foregoing methods of obtaining the K- $j\omega$ trace.

IV

CONCLUSION

The root locus technique is readily extendable into three dimensions. Projecting the three-dimensional root locus plot upon the K- $j\omega$ plane (for second-order systems) or upon the $\sqrt[q]{|K|}$ - $j\omega$ plane (for systems of any order) may be quickly and accurately accomplished to obtain the K- $j\omega$ trace of the three-dimensional locus. Closed-loop system response may then be evaluated from the K- $j\omega$ trace with regard to the variation of the imaginary part of complex roots with the root locus gain and with regard to sensitivity over any range of the root locus gain.

This paper develops and lists the rules for obtaining the K- $j\omega$ trace, the utilization of which requires only a knowledge of the pole-zero configuration of the open-loop transfer function. Several practical examples applying these rules are illustrated in chapters II and III.
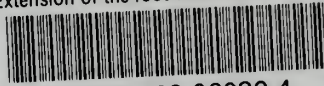
The use of the K- $j\omega$, trace provides another useful tool for the engineer in the design and analysis of feedback control systems.

BIBLIOGRAPHY

1. Clements, G. R. and Wilson, L. T., Manual of Mathematics and Mechanics. McGraw-Hill, 1947.

2. Smith, P. F., Gale, A. S., and Neeley, J. H., New Analytic Geometry, Revised Edition. Ginn and Co., 1956.

3. Thaler, G. J. and Brown, R. G., Analysis and Design of Feedback Control Systems. McGraw-Hill, 1960.

51